Remote sensing of vegetation and soil moisture content in Atlantic humid mountains with Sentinel-1 and 2 satellite sensor data

Antonio T. Monteiro [a,b,*], Salvador Arenas-Castro [c], Suvarna M. Punalekar [d], Mário Cunha [e,f], Inês Mendes [a], Mariasilvia Giamberini [b], Eduarda Marques da Costa [a], Francesco Fava [g], Richard Lucas [d]

[a] Centro de Estudos Geográficos (CEG), Laboratório Associado TERRA, Instituto de Geografia e Ordenamento do Território (IGOT), Universidade de Lisboa, Rua Edmée Marques, 1600-276 Lisboa, Portugal
[b] Istituto di Geoscienze e Georisorse, Consiglio Nazionale delle Ricerche, Via Moruzzi 2, 56124 Pisa, Italy
[c] Área de Ecología, Departamento de Botánica, Ecología y Fisiología Vegetal, Facultad de Ciencias, Universidad de Córdoba, Campus de Rabanales, 14014 Córdoba, Spain
[d] Department of Geography and Earth Sciences, University of Aberystwyth, Penglais, Aberystwyth SY23, United Kingdom
[e] Institute for Systems and Computer Engineering, Technology and Science (INESC TEC), Campus da Faculdade de Engenharia da Universidade do Porto, 4200-465 Porto, Portugal
[f] Sciences Faculty, Porto University, Rua do Campo Alegre, sn., 4169-007 Porto, Portugal
[g] Department of Environmental Science and Policy (ESP), Università degli Studi di Milano, 20133 Milan, Italy

ARTICLE INFO

ABSTRACT

The satellite monitoring of vegetation moisture content (VMC) and soil moisture content (SMC) in Southern European Atlantic mountains remains poorly understood but is a fundamental tool to better manage landscape moisture dynamics under climate change. In the Atlantic humid mountains of Portugal, we investigated an empirical model incorporating satellite (Sentinel-1 radar, S1; Sentinel-2 optical, S2) and ancillary predictors (topography and vegetation cover type) to monitor VMC (%) and SMC (%). Predictors derived from the S1 (VV, HH and VV/HH) and S2 (NDVI and NDMI) are compared to field measurements of VMC (n = 48) and SMC (n = 48) obtained during the early, mid and end of summer. Linear regression modelling was applied to uncover the feasibility of a landscape model for VMC and SMC, the role of vegetation type models (i.e. native forest, grasslands and shrubland) to enhance predictive capacity and the seasonal variation in the relationships between satellite predictors and VMC and SMC. Results revealed a significant but weak relationship between VMC and predictors at landscape level (R^2 = 0.30, RMSEcv = 69.9 %) with S2_NDMI and vegetation cover type being the only significant predictors. The relationship improves in vegetation type models for grasslands (R^2 = 0.35, RMSEcv = 95.0 % with S2_NDVI) and shrublands conditions (R^2 = 0.52, RMSEcv = 45.3 %). A model incorporating S2_NDVI and S1_VV explained 52 % of the variation in VMC in shrublands. The relationship between SMC and satellite predictors at the landscape level was also weak, with only the S2_NDMI and vegetation cover type exhibiting a significant relationship (R^2 = 0.28, RMSEcv = 18.9 %). Vegetation type models found significant associations with SMC only in shrublands (R^2 = 0.31, RMSEcv = 9.03 %) based on the S2_NDMI and S1_VV/VH ratio. The seasonal analysis revealed however that predictors associated to VMC and SMC may vary over the summer. The relationships with VMC were stronger in the early summer (R^2 = 0.31, RMSEcv = 90.1 %; based on S2_NDMI) and mid (R^2 = 0.37, RMSEcv = 70.8 %; based on S2_NDVI), butnon-significant in the end of summer. Similar pattern was found for SMC, where the link with predictors decreases from the early summer (R2 = 0.33, RMSEcv = 16.0 %; based on S1_VH) and mid summer (R2 = 0.30, RMSEcv = 17.8 %; based on S2_NDMI) to the end of summer (non-significant). Overall, the hypothesis of a universal landscape model for VMC and SMC was not fully supported. Vegetation type models showed promise, particularly for VMC in shrubland conditions. Sentinel optical and radar data were the most significant predictors in all models, despite the inclusion of ancillary predictors. S2_NDVI, S2_NDMI, S1_VV and S1_VV/VH ratio were the most relevant predictors for VMC

and, to a lesser extent, SMC. Future research should quantify misregistration effects using plot vs. moving window values for the satellite predictors, consider meteorological control factors, and enhance sampling to overcome a main limitation of our study, small sample size.

1. Introduction

In the mountain regions of Europe, emerging interplay of climate shift, anthropogenic activities and evolving policies have substantially impacted vegetation and soil moisture contents (herein referred to as VMC and SMC (%) respectively). These elements play pivotal roles in biodiversity, food security, carbon cycle, water supply, and in the well-being of human communities (Drenkhan et al., 2023; Gómez-Giráldez et al., 2014). Disruptions in VMC and SMC challenge long standing assumptions (i.e., mountains being endless water towers), traditions (i.e. fire being a fuel management tool) and practices (i.e. farming water use), particularly in Mediterranean regions (Pôças et al., 2011; Vij et al., 2021). Better management of VMC and SMC is therefore becoming paramount if the undesirable impacts on mountains and benefitting catchments are to be addressed (Costa-Saura et al., 2021; Lehmann et al., 2020). When accessibility, time and costs are impeditive to the use of direct measurement methods (i.e. time domain reflectometry (Santi et al., 2016), satellite remote sensing emerges as a viable alternative (Liang et al., 2021; Pace et al., 2021; Pôças et al., 2013; Schönbrodt-Stitt et al., 2021), requiring thorough evaluation.

Satellite remote sensing offers the opportunity to obtain spatially explicit information on landscapes at regular time intervals. Over the past decade, satellite data have contributed to significant advances in retrieving VMC (Forkel et al., 2023) and SMC (i.e., the Copernicus soil moisture; Bauer-Marschallinger et al., 2019). Common approaches for evaluating VMC and SMC across landscapes include physically-based and empirical models (Acharya et al., 2022), with the commonly preferred due the operation constraints of detailed parameterization in physically-based models (Forkel et al., 2023). Thus, empirical models that estimate moisture from indices derived primarily from optical data have been promoted as the most efficient and viable solution (Costa-Saura et al., 2021), and important developments in this approach continue to take place (i.e., through the PYSMM soil moisture toolbox; Greifeneder et al., 2021). Empirical moisture models have largely focused on the statistical relationship between field measurements of VMC or SMC and optical reflectance data (Yebra et al., 2013). This panorama is however changing with the increasing availability of data from Synthetic Aperture Radar (SAR) operating in the microwave portion of the electromagnetic spectrum, including C-band observations by the Sentinel-1 SAR (S1) (Santi et al., 2016). Because of their observational capabilities during day and night regardless of cloud conditions and their ability to penetrate a few millimetres beyond the top of the canopy, microwave measurements have the potential to allow systematic measurement of VMC and SMC (Konings and Saatchi, 2021). SAR data can be used either alone (Schlund and Erasmi, 2020; Schönbrodt-Stitt et al., 2021) or in synergy with optical reflectance data (Liang et al., 2021; Tanase et al., 2022; Wang et al., 2022).

In Mediterranean agroecosystems, Costa-Saura et al. (2021) demonstrated a strong link between Sentinel-2 (S2) optically-derived indices such as the Normalised Difference Moisture Index (NDMI) and VMC. Pace et al. (2021) in more humid Atlantic conditions suggested that the Normalized Difference Vegetation Index (NDVI) depicted the responses of riparian vegetation to water stress. In Chinese semi-arid agricultural landscapes, an empirical model composed by the Normalized Difference Water Index (NDWI) and short-wave infrared band (SWIR) based on S2 was the most accurate for VMC estimation (Wang et al., 2022). In Austrian crop conditions, and particularly for corn and winter cereals, Vreugdenhil et al. (2018) found that an exponential model based on the ratio of the backscatter coefficient in vertically (V) and horizontally (H) received backscatter (i.e., VH) and VV polarisations

could account for 87 % and 63 % of the variation in VMC. For SMC, the recent findings have less consensus. In American crop conditions, a very weak relationship between moisture related indices obtained from Landsat sensor data and surface SMC was reported by Acharya et al. (2022). In Mediterranean forest basins, concerns regarding the realism of the temporal evolution of SMC derived from S1 were also highlighted by Gomis-Cebolla et al. (2022), which concurred with the low agreement observed in areas dominated by forests with strong topography (Bauer-Marschallinger et al., 2019). The agreement between SMC and S1 appeared to increase over plain and agricultural areas (Bauer-Marschallinger et al., 2019). Schönbrodt-Stitt et al. (2021) also suggested that combining SAR and terrain parameters may help improve model accuracy.

Because mountains have always been viewed as endless water sources, empirical moisture models using satellite data are relatively scarce here. However, the large-scale water crisis observed in European mountains since 2018 (Stephan et al., 2021) rises the demand for timely as well as historical information on VMC and SMC from satellite-based monitoring over these critical regions. Satellite-based monitoring could be of support for instance for policy compliance (i.e. water use restrictions during droughts), risk mitigation (i.e. regulation of traditional man-made fuel management through fire; anticipation of livestock food insecurity) or climate change adaptation (i.e. understanding land system dynamics in climate change societies). Recent studies have been encouraging with these highlighting a strong link between the heterogeneity in the time-series of Planetscope NDVI and SMC in the Rocky mountains (Devadoss et al., 2020). Artificial Neural Network models (ANN) also accurately predicted SMC in the Himalayan Foreland (Singh and Gaurav, 2023), although overestimates of in-field observed SMC based on S1 retrievals were noted in the Iberian mountains (Carvalho-Santos et al., 2018).

This study evaluated S1 and S2 satellite data for monitoring VMC and SMC in Southern European Atlantic humid mountains. The goal was twofold: a) to explore an empirical model incorporating satellite-based predictors to estimate VMC and SMC with this then providing a potential contribution to the management of landscape moisture dynamics, and b) reduce the knowledge gap in this regard in Southern European Atlantic humid mountains (Rodriguez-Jimenez et al., 2023). Here, innovative landscape management tools have become highly necessary for coping with increasing hydroclimatic anomalies that threaten the well-being of people and ecosystems (Choler, 2023). Hence, the establishment of a model for landscape moisture prediction would be a valuable additional resource, particularly if that model informed by i.e. local field data of VMC for the dominant vegetation types and S1 or S2 predictors would be able to deliver i.e. accurate spatial-explicit VMC estimates. This one size fits all concept has great significance for usages that goes beyond the remote sensing community.

In the study, four major questions were established: (1) To what extent do S1 radar and S2 optical data and/or derived indices relate to VMC and SMC? (2) Can a generalised landscape model be established to quantify VMC and SMC from these data (3) Can model performance be improved by considering specific vegetation type models? and (4) Are any relationships observed stable over time?

To address these questions were considered the relationships between i) S1 data (VH, VV, VV/VH ratio) and ii) S2 indices (NDVI, NDMI) and a dataset of 96 field measurements of VMC (n = 48) and SMC (n = 48) taken in native forests, shrublands and grasslands in the S1 overpass days throughout the summer of 2016.
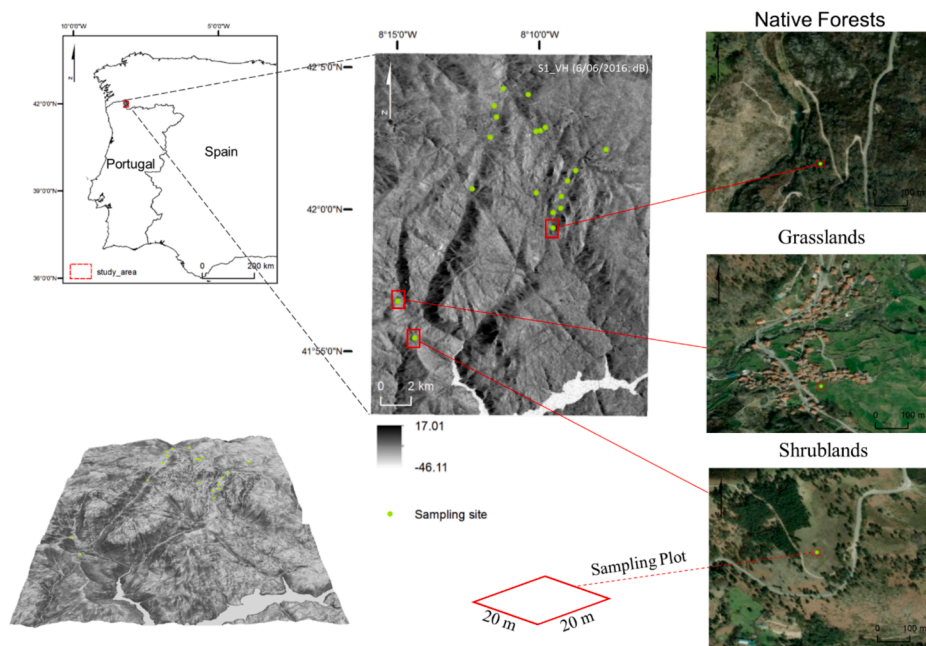
Fig. 1. Location of the study in the Portuguese Peneda-Gerês mountain, Gerês-Xurez Transboundary Biosphere Reserve. The upper central panel shows the study area captured by the VH backscatter coefficient of S1 on the 6th June 2016 and the location of the plots surveyed for VMC and SMC during the study period (in green, n = 19). The lower central panel shows the size of the sampling plot used (20 x 20 m). The panels on the right exemplify the characteristics of predominating vegetation types in the area surveyed: native forests grasslands; shrublands. (For interpretation of the references to colour in this figure legend, the reader is referred to the web version of this article.)

Table 1
The set of sampling plots (see Fig. 1) and their attributes in terms of vegetation type, altitude, slope (º), aspect (º), and the dominating species. Native forests (N), Grasslands (G), Shrublands (S).

Plot Number	Vegetation Type	Altitude (m a.s.l)	Slope (°)	Aspect (°)	Exposition	Dominating species
1	N	811	20.16	268	W	*Quercus pyrenaica; Quercus robur*
2	S	898	8.01	268	W	*Pterospartum cantabricum; Ulex europaeus; Erica Umbellata; Erica autralis*
3	N	853	7.69	198	S	*Quercus pyrenaica; Quercus robur*
4	G	881	5.31	262	W	*Agrostis capillaris; Plantago lanceolata; Ranunculus repens;*
5	N	932	4.57	255	W	*Quercus pyrenaica; Quercus robur; Salix atrocinerea*
6	G	1020	7.75	167	S	Unknown grass
7	S	1239	8.6	177	S	*Pterospartum cantabricum; Ulex europaeus; Erica Umbellata;Erica arborea*
8	N	864	15.66	104	E	*Quercus pyrenaica; Quercus robur*
9	G	1014	1.91	180	S	Unknown grass
10	S	1051	7.59	18	N	*Calluna vulgaris; Erica Umbellata; Ulex minor;*
11	S	1074	10.11	187	S	*Cytisus striatus*
12	S	1106	16.4	323	NW	*Cytisus striatus*
13	G	915	8.86	11	N	Unknown grass
14	S	1043	12.56	138	SE	*Ulex europaeus; Erica Umbellata; Erica autralis; Erica arborea;*
15	N	962	6.16	129	SE	*Betula alba*
16	S	928	1.51	148	SE	*Ulex minor; Erica arborea;Agrostis castellana; Erica autralis; Festuca Iberica*
17	N	913	9.48	150	SE	*Betula alba*
18	G	638	9.48	117	SE	*Lolium perenne; Ranunculus repens; Plantago lanceolata*
19	S	917	13.37	124	SE	*Pterospartum cantabricum; Ulex minor; Erica Umbellata; Erica arborea*

2. Methods

2.1. Study area

The study area is located in the northern Portugal at Peneda-Gerês mountain range, Iberian Peninsula (31110 ha, 41°42′25.2″ N, 8°10′1.2″ W, Fig. 1). This mountain range has a significant role in the Portuguese water catchment context. Elevation ranges from 145 to 1253 m above sea level (a.s.l), and the topography is complex. The site is a traditional mountain pastoral landscape affected by land abandonment. It is renowned for its natural and cultural heritage, namely containing the last remaining native forest ecosystem with reduced human influence that enclose man-made farmland mosaics (Monteiro et al., 2021). The landscape is mainly comprised of fragments of deciduous forests, shrublands, and permanent hay meadows. Native oak forests (Habitat 9230 listed in the Habitats Directive 92/43/EEC) and permanent hay meadows (Habitat 6510) are two main conservation priorities. The current forces shaping the landscape are the regrowth of oak forests and the spread of shrubs into areas that were once farmland. Wildfires are important, with the frequency of vegetation burns generally being greatest in the summer months (Calheiros et al., 2022). The climate is temperate oceanic (Rivas-Martínez et al., 2017) and there is a large amplitude of values (from −10 to 35 °C from a mean of 13 °C) and hence differences in temperature between the winter and summer seasons. The annual mean precipitation amounts to 1500 mm/year (Carvalho-Santos et al., 2016). Distributed along the autumn (39.1 %), winter (31.5 %)

Table 2

Calendar of on-site vegetation and soil moisture measurements and specifications of Sentinel-2 and Sentinel-1 satellites overpass in the Peneda-Gerês mountain range. CET stands for Central European Time.

Time (year of 2016)	On-site Dates	Sentinel-2 Overpass	Sentinel-1A Overpass				
			Day of acquisition	Time of acquisition (CET)	Relative orbit number	Incidence angle over the study area	Pass
Early Summer	6-7th June	2nd June	6th June	18:27h33s	147	38.25° to 39.28°	Ascending
Mid Summer	12–13th July	9th July	12th July	18:27h35s	147	38.25° to 39.28°	Ascending
End of Summer	21–22th September	20th September	22th September	18:27h38s	147	38.25° to 39.28°	Ascending

and spring (27.5 %) seasons. The region is also characterized by long periods with high frequency of frost occurrences. In 2016, intense precipitation (compared to historical mean from 1971 to 2000) occurred in the late spring and early summer (May, 400 mm, +300 %; June, 100 mm, +75 %, Atmosfera, 2016).

2.2. Field data collection

A field campaign was conducted in 19 sites during the summer of 2016 to obtain vegetation moisture content (VMC) and soil moisture content (SMC). Collection of VMC and SMC data was carried out in the early summer (6-7/06/2016), mid summer (12-13/07/2016) and end of summer (21-22/09/2016) performing in total six days of field data collection. A set of 114 field measurements were obtained (VMC, n = 57; SMC, n = 57). After laboratory processing and data quality check (see details below), the dataset retained for analysis was composed by 96 measurements (VMC, n = 48; SMC, n = 48). Table 1 provides descriptions for all the sites given in Fig. 1. Dominating species refers to plant species that cover most of the sampling unit. In specific, each collection date (i.e. early summer) consisted of a two-days field survey starting at 10:00 h and ending at 17:00 h. The first day of field survey was always coincident with the Sentinel-1 overpass day in the study area, except for the collection date at the end of the summer (21-22/09/2016). In the end of the summer, S1 overpass occurred in the second day of field data collection. The location of the surveyed sites was a compromise between the representativeness of the vegetation type, geographical distribution in the study area and easy accessibility. Each surveyed site was at least 50x50 m^2 large and homogeneous in terms of vegetation cover type (i.e. native forests, shrublands and grasslands). The altitude of the sites ranged from 638 to 1239 m a.s.l.

VMC and SMC were measured using destructive sampling. In each surveyed site, a sampling unit of 20x20 m^2, homogeneous in terms of overhead vegetation fractional cover, species composition and canopy height, was established. Next, to obtain VMC in grasslands and shrublands, the ground vegetation was harvested in a 0.5x0.5 m^2 quadrat using a handheld mower, and a representative sample composed of the dominating species collected. In native forest sampling units, only leaves were collected at north, south, east, and west exposures using a clipper. All the samples were stored in a waxed paper bag. For SMC, a soil sample for the first 10 cm was collected in the non harvested area of the sampling unit using a footstep soil probe (SoilIsMPLR series- Martin Lishman) and stored in an aluminium soil sample box (120 cc). The decision to collect at 10 cm depth was related to the sensitivity of SAR data to soil moisture in the top 5–10 cm of soil (El Hajj et al., 2017; Feldman et al., 2023; Jackson et al., 1984). Using a digital scale, all vegetation and soil samples were weighed directly in the field to avoid water loss and stored in a portable cooler bag for transportation. Twigs and leaves were weighed together in the shrublands, but for native forest samples, only the leaves were gathered and weighed. On return to the laboratory, the vegetation samples were oven dried for 48 h at 70 °C (Brown et al., 2022) whilst the soil samples were oven dried for 48 h but at 105 °C (Holzman et al., 2017). VMC and SMC were estimated in percentage on a dry-weight basis for the collected sample (at vegetation type level) using Equation (1), where FW is the fresh weight measured in the field and DW

represents the oven dry weight of the same sample. Following laboratory processing of the VMC and SMC, a quality check round was undertaken, which resulted in the exclusion of three plots from early (8,15,18), mid (4, 11, 12) and end of summer (4,11,12) due to inconsistencies in the data. The final dataset (n = 96) was composed by 16 observations for VMC and SMC in each collection data (early summer, 6-7th June; mid summer, 12-13th July; end of summer 21st – 22nd September), performing a total of 48 observations for each moisture variable.

$$Sample\ moisture (\%) = \left(\frac{(Fw - Dw)}{Dw} \right) * 100 \qquad (1)$$

2.3. Copernicus satellite imagery collection and processing

2.3.1. Sentinel-1

The S1 is a satellite mission from the European Space Agency (ESA) equipped with a C-band Synthetic Aperture Radar (SAR, 5.405 GHz, 5.6 cm wavelength) with both VV (vertical transmit and vertical receive) and VH (vertical transmit and horizontal receive) polarizations. Here, the data was obtained from the Copernicus Data Space Ecosystem (https://dataspace.copernicus.eu/) in the format of Level-1 Interferometric Wide (IW) Ground Range Detected (GRD), and a spatial resolution is 5 m × 20 m. To obtain the S1 backscatter (σ^0), each image was processed within the ESA's Sentinel Application Platform (SNAP V6.0, European Space Agency, Benninga et al., 2020) in the sequence of (1) apply orbit file, (2) thermal noise removal, (3) radiometric calibration, (4) speckle filtering (Lee filter), (5) range Doppler terrain correction, and (6) conversion to radar backscattering coefficient (σ∘) in decibels (dB). Three S1A radar backscattering images (Table 2) of the ascending pass with a local overpass time of 18:27 h were used to create three predictor variables for VMC and SMC, namely VV (referred to as S1_VV) and VH (S1_VH) backscatter coefficients and the ratio of VV and VH polarisation (S1_VV_VH_ratio). S1_VV/VH ratio was calculated as the difference between VV and VH, since it was calculated in decibels [dB] (Schlund and Erasmi, 2020). Because of VV and VH have different sensitivities to soil and vegetation moisture (Rao et al., 2020), we hypothesized that S1_VV/VH ratio could highlight the heterogeneity typical of Mediterranean vegetation types and thus benefit model estimates. The S1 acquired data on the 6th June, 12th July and 22St September 2016 coincided with the first day of field survey in the collection dates of early summer and mid summer, and with the second day of field survey in the collection date of the end of summer, respectively (see section 2.2.). The ascending pass was selected as the VMC has a strong diurnal cycle during the summer season (Konings and Saatchi, 2021) and we assumed that our data collected between 10:00 and 17:00 h would be more related to the S1 backscatter image captured at 18:27 h than to the descending pass at 06:33 h due of moisture depletion during the sampling period. Lastly, to match the spatial resolution of the S2 optical images (Section 2.3.2), the S1 images were resampled to 10 m using a bilinear interpolation approach and registered for UTM-WGS84 Zone 23 N reference frame.

2.3.2. Sentinel-2

Three cloud-free S2 Level 1C images (S2A MSI L1C, T29TNG tile) of the study area were acquired on 2nd June, 9th July and 20th September
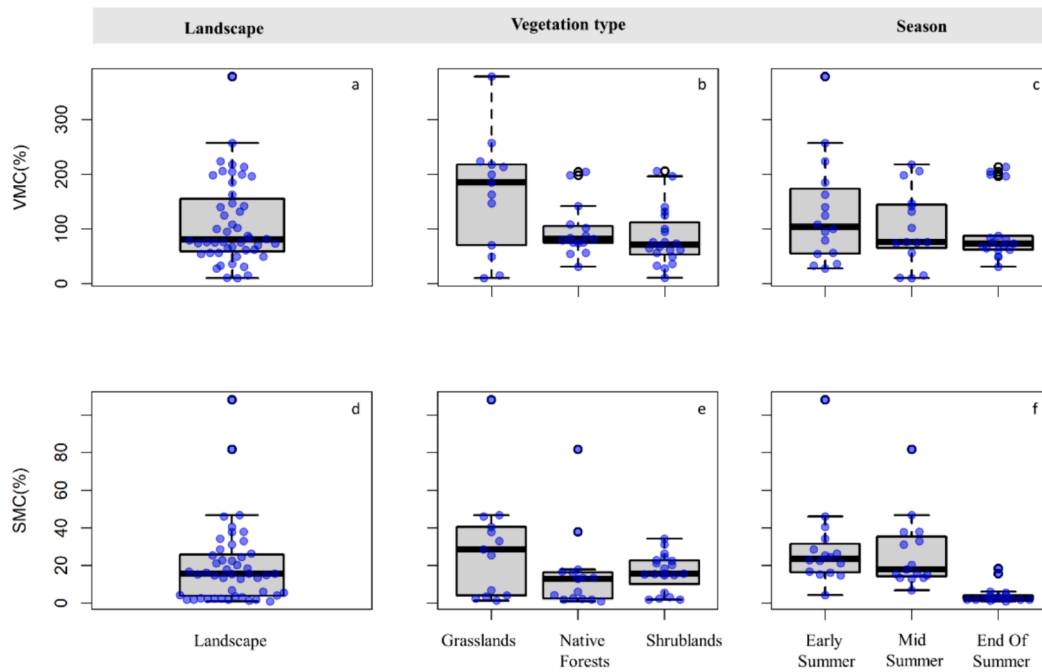
Fig. 2. Boxplots of VMC (top) and SMC (bottom) in percentage at the landscape level (a,d) and the variation across the different vegetation types (b,e) and during the season of field collection (c,f). The midline in a boxplot represents the median; the lower and upper box edges represent the 25th and 75th percentiles; the maximum and minimum values are represented by whiskers; and points beyond the whiskers indicate outliers.
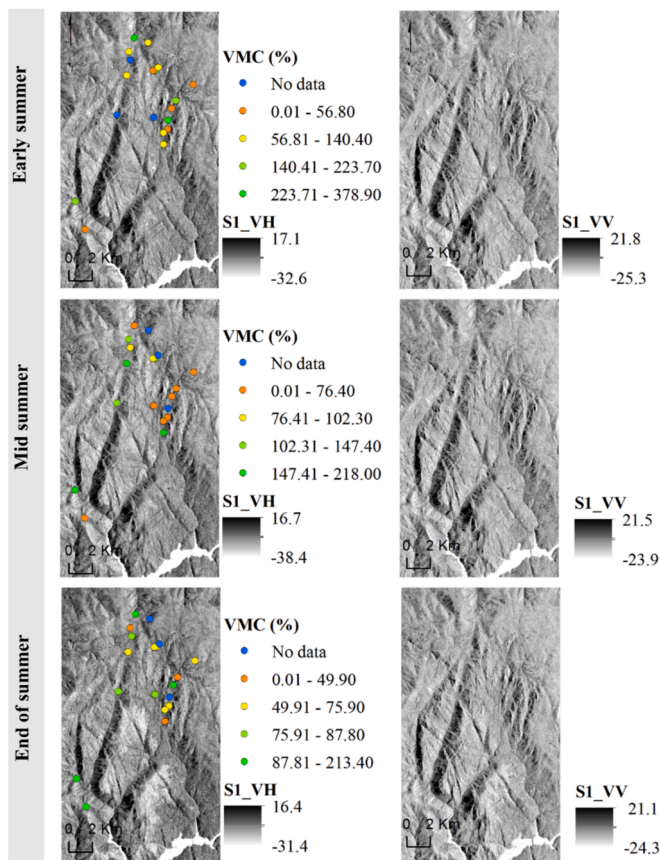

Fig. 3. Map showing the distribution of VMC (%) measured in the sampling sites in the early (6/07/2016), mid (12/07/2016), and end of summer (22/09/2016), and the Sentinel-1 VH and VV backscatter coefficients in decibels.

2016. These images were the closest in time to the date of the field campaigns (Table 2). S2 supports a multispectral optical sensor and the acquired imagery are provided free of charge by the European Space Agency (ESA). Each image comprises thirteen spectral bands and the spatial resolution ranges from 10 m or 20 m to 60 m depending upon the spectral region considered. S2 Level 1C data was downloaded through the United States Geological Survey (USGS) EarthExplorer (EE) user interface (https://earthexplorer.usgs.gov/) and pre-processed with the Sen2Cor software (Costa-Saura et al., 2021) to achieve the S2 Level 2A or Bottom-Of-Atmosphere (BOA) corrected reflectance images. Sen2Cor executes the atmospheric, terrain and cirrus correction of the Top-Of-Atmosphere (TOA) S2 Level 1C input data. Sen2Cor was parameterized to release S2 Level 2A outputs at 10 m spatial resolution (Pace et al., 2021) registered to the UTM-WGS84 Zone 23 N. Next, the red (b4, 665 nm, 10 m), near-infrared (NIR; b8, 842 nm, 10 m) and short wave infrared (SWIR; b11, 1610 nm, 20 m) were accessed as these allowed calculation of two optical predictor variables related previously to VMC and SMC (Costa-Saura et al., 2021; Liang et al., 2021; Rao et al., 2020): NDVI (S2_NDVI, Equation (2) and NDMI (S2_NDMI, Equation (3). NDVI and NDMI were estimated in Python using the osgeo, rasterio and numpy libraries.

$$NDVI = \frac{(NIR - RED)}{(NIR + RED)} \qquad (2)$$

$$NDMI = \frac{(NIR - SWIR)}{(NIR + SWIR)} \qquad (3)$$

2.4. Topographic data

Schönbrodt-Stitt et al. (2021) suggested combining topographic parameters with S1 data to improve the single SAR-based model for SMC retrieval in Mediterranean agroforestry systems. Slope and aspect were therefore included in the set of predictor variables and act as control factors for topographical effects. Both were derived from the Copernicus 30 m Digital Elevation Model (DEM) dataset (Airbus, 2020), which was resampled to 10 m resolution using a bilinear interpolation approach. To
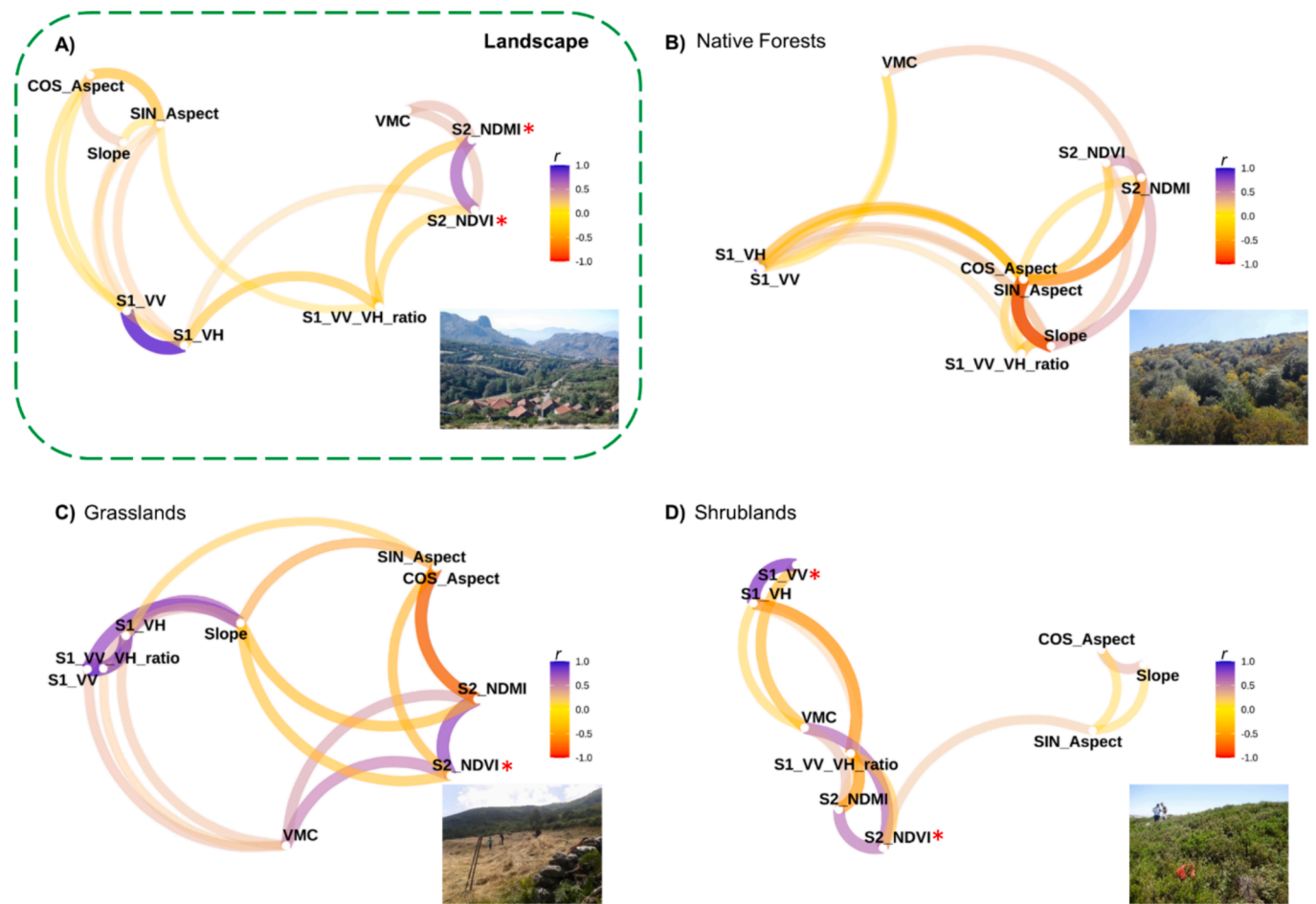
Fig. 4. Correlation network plot including all the Spearman correlations (*r*) between vegetation moisture content (VMC) and the predictor variables at landscape level (full dataset (n = 48), A), and across each vegetation type (native forests (n = 15), B; and grasslands (n = 13), C, shrublands (n = 20), D). Predictor variables that are more highly correlated with VMC appear closer, joined by large path thicknesses, coloured towards blue or red in case of positive or negative direction of the correlation, respectively. Predictor variables significantly associated with VMC (p < 0.05) are signed as *. (For interpretation of the references to colour in this figure legend, the reader is referred to the web version of this article.)

enable statistical analysis, the circular variable aspect was converted into a north–south (Northness) and east–west (Eastness) gradient, respectively, using the cosine and sine functions (Monteiro et al., 2013). All procedures were performed in QGIS version 3.24 (QGISTeam, 2022).

2.5. Approaches to retrieval of VMC and SMC

In view of a model for monitoring VMC and SMC under the conditions prevailing in Atlantic humid mountains characterised by Peneda-Gerês, we evaluated the relationship between field measurements of VMC and SMC and a set of satellite and ancillary predictors. VMC and SMC were the response variables. The prediction dataset included the S1 backscattering in decibels (S1_VV and S1_VH) and the ratio VV/VH (S1_VV_VH_ratio), the S2-derived NDVI (S2_NDVI) and NDMI (S2_NDMI), the topographic parameters (slope and aspect) and the vegetation cover type of the sample site (categorical variable used only in the models at landscape level).

In specific, at spatial level we tested the establishment of a generalized landscape level moisture model and the improvement in model performance by considering specific vegetation type models. At temporal level, we analysed the seasonal variation of the relationships between satellite predictors and VMC and SMC. The hypothesis of a generalized landscape level moisture model was measured using the entire dataset of each response variable (n = 48) composed by the field measurements obtained in native forest, grasslands and shrublands. We

assumed that these vegetation types together represent the key characteristics of the Southern European Atlantic humid mountains. To evaluate the effect of vegetation type models in model performance, we analysed the relationships between response and predictor variables using the dataset of each vegetation type (native forests, n = 15; shrublands, n = 20; grasslands, n = 13). To evaluate the seasonal variation of the relationships, we assessed the relationships between response and predictor variables using the dataset of each collection date (early summer, n = 16; mid summer, n = 16; end of summer, n = 16).

To link the predictor variables to VMC and SMC, a correlation network analysis followed by linear regression models with leave-one-out cross-validation (LOOCV) were applied (Fava et al., 2009). Correlation network analysis was based on the Spearman's Rank Correlation, which identified the set of variables having a significant correlation with VMC and SMC (*p* < 0.05) and collinearity among the predictor variables (r > 0.65). The set of significant predictor variables identified was then included in a linear regression model evaluating the capacity to predict VMC and SMC. The performance of the linear models was assessed by LOOCV as the dataset is small (i.e. VMC full dataset, n = 48) and the traditional data splitting (i.e.70/30) would not be truly representative of the overall dataset (Meyer et al., 2017). LOOCV delivers unbiased estimates for in-sample predictive accuracies but does not allow performance for predictions outside the spatial range covered by the dataset to be assessed (Wenger and Olden, 2012). The performance metrics were
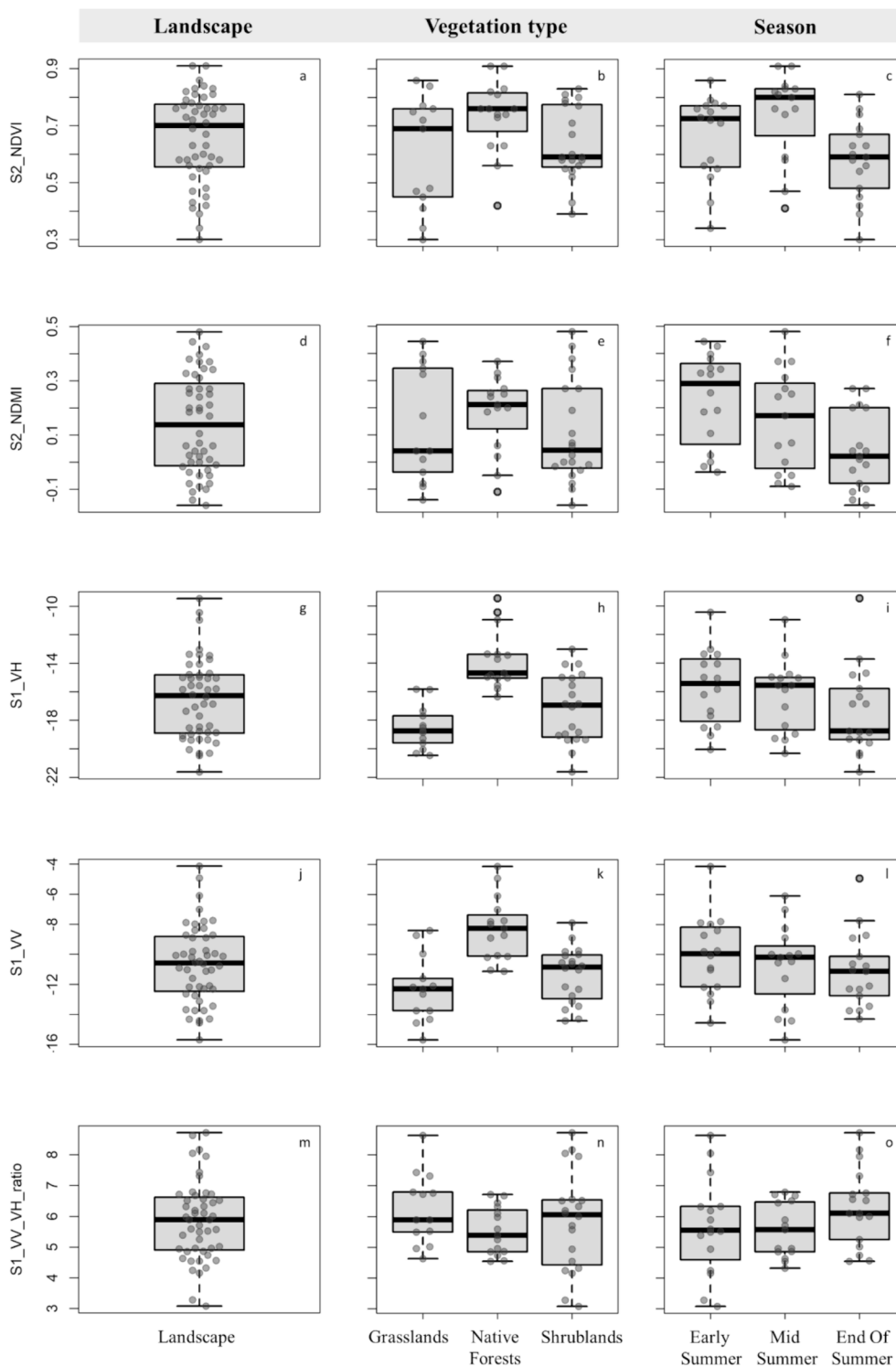
Fig. 5. Boxplots for the satellite variables selected to predict vegetation (VMC) and soil (SMC) moisture content in percentage at the landscape level (a, d, g, j, m), across vegetation types (grasslands; native forests; shrublands) and over the season (c, f, i, l, o). The midline in a boxplot represents the median; the lower and upper box edges represent the 25th and 75th percentiles; the maximum and minimum values are represented by whiskers; and points beyond the whiskers indicate outliers.

the coefficient of determination (R^2) and the cross-validated root mean squared error ($RMSE_{CV}$).

This statistical procedure was performed separately for VMC and SMC. The linear model stage was not performed as there was no significant correlation between dependent and predictor variables. To avoid model overfitting by including more predictor variables than allowed by the sample size, the maximum number of predictor variables in each linear model corresponded to one tenth of the number of observations used (Fieberg and Johnson, 2015). The predictor with strongest correlation coefficient was used to formulate the linear models where the sample size allowed only the inclusion of a single predictor (i. e. early summer model) All operations were performed using the packages Corrr, Hmisc, Caret, Tidyverse, Leaps, ggplot in the R statistical environment (RStudioTeam, 2020).

Table 3
Regression models for vegetation moisture content (VMC) and soil moisture content (SMC) as a function of spatial scale: landscape (full dataset, n = 48) and vegetation type (native forests, n = 15; grasslands, n = 13; shrublands, n = 20).

Model	Model Structure (Coefficient, SE)	Df	Intercept	P-value	R^2	R^2_{CV}	$RMSE_{CV}$ (%)
Landscape	VMC ~ S2_NDMI (135.66, 54.00) + Veg_type Native forests (−73.05, 25.14) + Veg_type Shrublands (−75.36, 23.58)	46	145.35 ± 19.76	0.001	0.30	0.16	69.9
	SMC ~ S2_NDMI (51.01, 14.71.00) + Veg_type Native forests (−16.54, 6.85) + Veg_type Shrublands (−11.69, 6.43)	46	22.52 ± 5.39	0.002	0.28	0.15	18.9
Native forests	VMC~	–	–	n.s	–	–	–
	SMC~	–	–	n.s	–	–	–
Grasslands	VMC ~ S2_NDVI (315.86, 128.86)	11	−26.47 ± 81.5	0.03	0.35	0.17	95.0
	SMC~	–	–	n.s	–	–	–
Shrublands	VMC ~ S1_VV (−14.96, 4.83) + S2_NDVI (164.13, 69.11)	17	−189.02 ± 63.80	0.001	0.52	0.36	45.3
	SMC ~ S2_NDMI (15.53, 12.57) + S1_VV_VH_ratio (−17.50, 13.70)	17	41.44 ± 21.86	0.04	0.31	0.11	9.03

Note: Standard Error (SE), Degrees of freedom (df), R squared (R^2), cross-validated coefficient of determination (R^2_{CV}) and cross-validated root mean squared error ($RMSE_{CV}$ in percentage).

3. Results

3.1. Spatio-temporal dynamics of VMC and SMC

At the landscape level, the VMC ranged from 10.3 % to 378.9 %, with a median of 80.5 % (Fig. 2-a) indicating a large heterogeneity in vegetation moisture between sites (Fig. 3) At vegetation type level, the highest VMC variability was associated with the grasslands sites, ranging from 10.3 % to 378.9 % (with a median of 185.1 %; Fig. 2-b). In the native forest sites, a lower amplitude was observed as the range was from 31.4 % to 204.6 % (median of 81.7 %). Shrubland sites had a median VMC of 71.1 % and a range from 10.9 % to 205.6 %. At seasonal level, the median VMC decreased from 104.2 % to 76.2 % and then to 74.9 % from early to mid and late summer respectively. At the landscape level, SMC ranged from 0.86 % to 108.1 % (median of 15.6 %; Fig. 2-d). As with the VMC, grasslands exhibited the highest SMC variability, ranging from 1.2 % to 108.1 % (median of 28.6 %; Fig. 2-e). The SMC range of native forest sites was narrower (0.9 % to 81.7 %) and the median of 12.9 % was the lowest among the three vegetation types. For the shrubland sites, the SMC values ranged from 1.8 % to 15.6 % (median of 15.7 %). As with the VMC, the median SMC decreased from 23.6 %, to 16.6 % and then to 2.4 % from early to mid and late summer respectively; Fig. 2-f).

3.2. Satellite-based predictive model of VMC

Among the predictor variables analysed (satellite, topographic and vegetation cover type), only the satellite-based and vegetation cover type variables demonstrated a significant relationship with VMC, which varied both spatially and temporally. At the landscape level, most predictor variables have correlation values below 0.65, except for S2_NDMI and S2_NDVI (r = 0.68), S1_VH and S1_VV (r = 0.87). To address this collinearity issue, the S2_NDVI and S1_VV were excluded from the analysis (Fig. 4-A and Supplementary Fig. S1-A). Correlation network analysis revealed that S2_NDMI was the only satellite variable showing a significant moderate relationship with VMC (r = 0.40, p = 0.005). S2_NDMI, which ranged from −0.16 to 0.48 (Fig. 5-d), displayed a positive association with VMC, indicating that sites with higher NDMI values tended to have higher VMC values. A linear model based on S2_NDMI and vegetation cover type explained 30 % of the variation in VMC (R^2 = 0.30, RMSEcv = 69.9 %; Table 3 and Fig. 5-a). None of the S1 or topographic predictors were related to VMC (p > 0.05).

Interestingly, the strength of the relationship with VMC improved when analysed at the vegetation type level, with the exception of native

forests where the relationships were non-significant (Fig. 4-B, Table 3 and Supplementary Fig. S2-A). In grasslands, there was a significant moderate association between VMC and the S2_NDVI (r = 0.57, p = 0.04; Fig. 4-C and Supplementary Fig. S2-B). A linear model based on S2_NDVI accounted for 35 % of the variation in VMC (R^2 = 0.35, RMSEcv = 95 %; Table 3 and Fig. 6-e). The S2_NDVI ranged from 0.30 to 0.86 (Fig. 5-b). The positive relationship between the S2_NDVI and VMC suggests that the former increases with VMC. However, it was in shrublands that the strongest relationship between satellite predictors and VMC was found. VMC correlated strongly with S2_NDVI (r = 0.64, p = 0.002) and moderately with S1_VV (r = -0.47, p = 0.04, Fig. 4-d and Supplementary Fig. S2-C). A model based on these variables explained 52 % of the variation in VMC across the sampling sites (R^2 = 0.52, RMSEcv = 45.3 %, Table 3 and Fig. 6-c). A positive relationship between the S2_NDVI and VMC in shrublands was observed with NDVI values ranging from 0.39 to 0.83 (Fig. 5-b). In contrast, VMC has a negative relationship with S1_VV backscatter coefficient. The S1_VV values ranged from −14.4 dB to −7.9 dB with a median value of −10.8 dB.

The seasonality of the relationships was assessed by analysing the relationship between VMC and the predictor variables in each collection date (early, mid and end of summer). The comparison of the VMC relationships indicated that the relationships were not stable over the summer season. They varied in terms of predictors associated to VMC and predicting capacity. In the early summer, VMC correlated strongly with S2_NDMI (r = 0.61, p = 0.05) and moderately with S1_VH (r = -0.53, p = 0.05, Fig. 7-A and Supplementary Fig. S3-A). Both predictors could integrate a VMC model, but our sample size (n = 16) allowed only the inclusion of a single predictor. A linear model based on S2_NDMI, strongest predictor, explained 31 % of the variation of VMC (R^2 = 0.31, RMSEcv = 90.1 %, Table 4 and Fig. 11-a). In mid summer the predicting capacity expanded slightly (R^2 = 0.37, RMSEcv = 70.8 %, Table 4 and Fig. 11-b) based on a moderate positive correlation between VMC and S2_NDVI (r = 0.57, p = 0.05, and Supplementary Fig. S3-B). At the end of the summer season (Fig. 7-C, Table 4 and Supplementary Fig. S3-C) no significant relationships were found to VMC.

3.3. Satellite based predictive model of SMC

Satellite and vegetation cover type predictors were found to be the only variables linked to SMC spatially and temporally. Fig. 8 maps the distribution of SMC in the surveyed sites. Fig. 9 provides the network correlation plots illustrating the significant relationships at landscape and vegetation type level. Fig. 10 illustrate the significant relationships at temporal level or by the season of data collection. Further details for
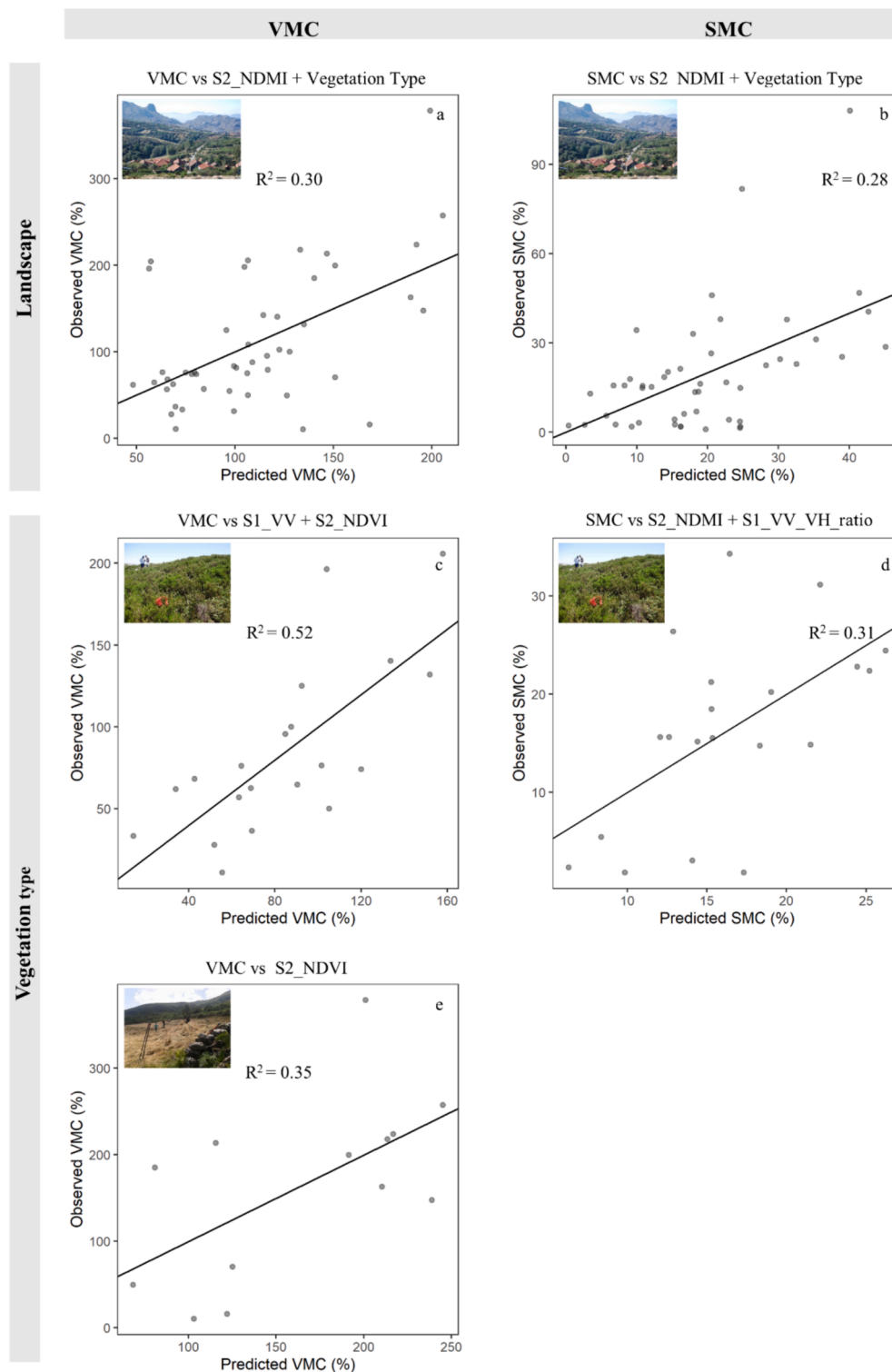
Fig. 6. Predicted and observed vegetation moisture content (VMC, %) and soil moisture content (SMC, %) using the regression models established with the predictors significantly correlated with VMC and SMC at landscape level and by vegetation type. VMC and SMC at landscape level predicted using the S2_NDMI and vegetation cover type, respectively (a, b); VMC for shrublands predicted using the S1_VV backscattering and S2_NDVI (c); SMC for shrublands predicted using the S2_NDMI and S1_VV_VH_ratio (d). VMC for grasslands predicted using the S2_NDVI (e). Coefficient of determination (R^2).

the relationships are provided in the Supplementary Figs. S1, S2, S3. At the landscape level (n = 48), both the S2_NDMI (r = 0.44, p = 0.002) and S2_NDVI (r = 0.30, p = 0.04) were moderately correlated with SMC (Fig. 9-A and Supplementary Fig. S1-B). However, due to their strong correlation (r > 0.65), S2_NDVI was excluded from the analysis. A model based on the S2_NDMI and vegetation cover type explained 28 % of the

variation in SMC (i.e, R^2 = 0.28, RMSEcv = 18.9 %; Table 3 and Fig. 6-b). S2_NDMI was positively associated with SMC. Sites with large NDMI values presented large SMC values.

At the vegetation type level, the strength of the link with SMC did not improve and the only areas where a significant relationship with SMC was found were shrublands (Fig. 9-D and Supplementary Fig. S2-4). SMC
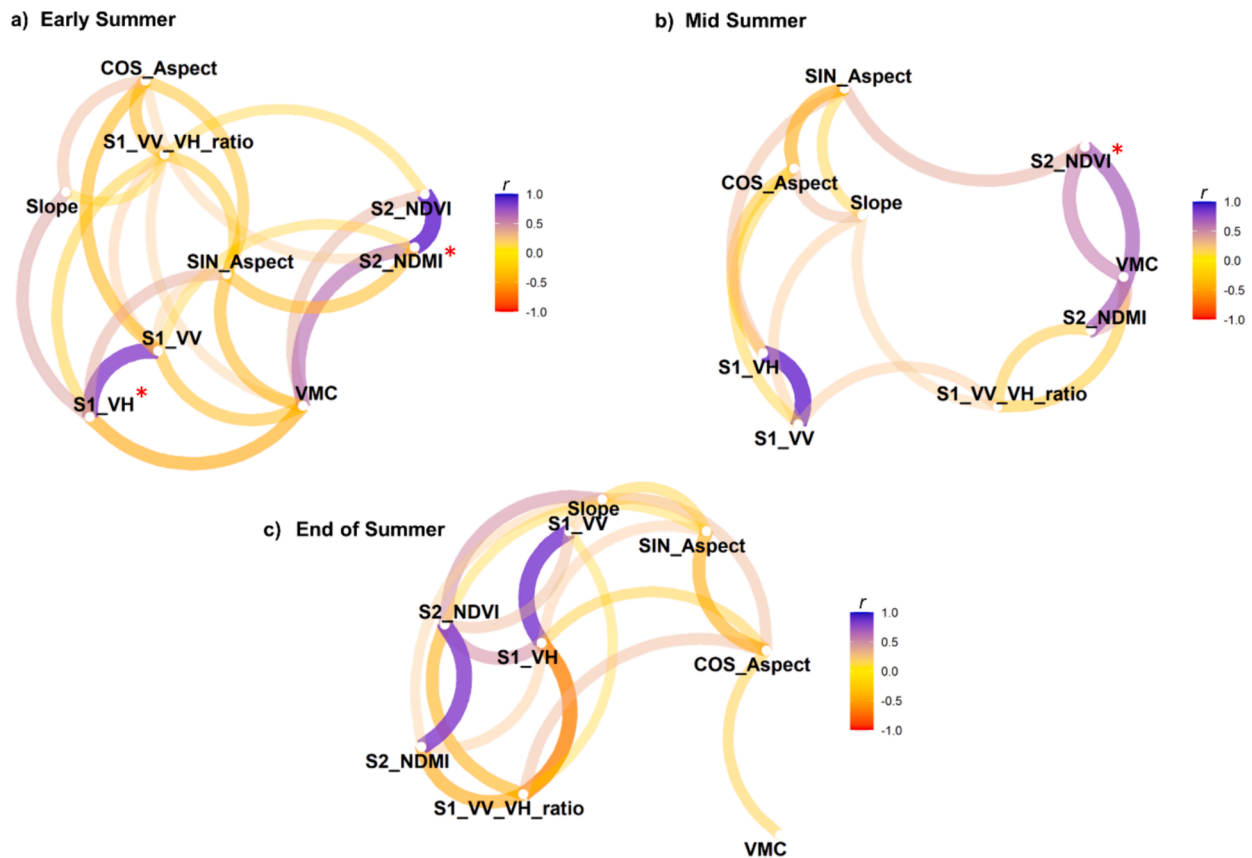
Fig. 7. Correlation network plot including all the Spearman correlations (*r*) between vegetation moisture content (VMC) and the set of predictor variables grouped by time: early (6-7th June, n = 16, A), mid (12-13th July, n = 16, B) and end (21st-22nd September, n = 16, C) of summer 2016. Predictor variables more highly correlated with VMC appear closer, joined by large path thickness coloured towards blue or red in case of positive or negative directions of the correlation, respectively. Predictor variables significantly associated with VMC (p < 0.05) are signed as *. (For interpretation of the references to colour in this figure legend, the reader is referred to the web version of this article.)

Table 4
Regression models for vegetation moisture content (VMC) and soil moisture content (SMC) as a function of time (early (6-7th June), mid (12-13th July) and late (21st and 22nd September,) summer 2016.

Model	Model Structure (Coefficient, SE)	df	Intercept	P-value	R^2	R^2_{CV}	$RMSE_{CV}$ (%)
Early Summer	VMC ~ S2_NDMI (313.58, 125.6)	13	56.91 ± 35.44	0.02	0.31	0.11	90.1
	SMC ~ S1_VH (−5.09, 1.94)	14	−50.91 ± 30.88	0.02	0.33	0.07	16.0
Mid Summer	VMC ~ S2_NDVI (261.88, 91.99)	14	−89.50 ± 68.13	0.01	0.37	0.14	70.8
	SMC ~ S2_NDMI (54.39, 22.02)	14	18.29 ± 5.09	0.03	0.30	0.10	17.8
End of Summer	VMC~	–	–	n.s	–	–	–
	SMC ~ S2_NDVI (−2.90, 7.82)	13	5.40 ± 4.67	n.s	0.22	0.02	4.74

Note: Standard Error (SE), Degrees of freedom (df), R squared (R^2), cross-validated coefficient of determination (R^2_{CV}) and cross-validated root mean squared error ($RMSE_{CV}$ in percentage).

in native forest and grassland conditions were not significantly correlated with any predictor variables (p > 0.05). SMC in shrublands was related to S2_NDMI (r = 0.53, p = 0.02) and S1_VV_VH_ratio (r = −0.46, p = 0.04). A model based on these variables explained 31 % of the variation in SMC (R^2 = 0.31, RMSEcv = 9.03 %; Table 3 and Fig. 6-d). In shrublands, S2_NDMI ranging from −0.16 to 0.48 (Fig. 5-e) increases in sites with higher SMC. The S1_VV_VH_ratio, which ranged from 3.1 dB to 6.53 dB, was larger in sites with lower SMC.

Regarding the seasonality of the relationships, a trend could not be discerned. Predicting capacity and predictors associated to SMC varied with the season. The relationship was more robust in the early summer and mid summer, but no significant models were identified in the late summer (Fig. 10 and Table 4). In the early summer, SMC was moderately correlated with S1_VH (r = 0.61, p = 0.05) and S1_VV (r = −0.53, p = 0.05, Fig. 10-A and Supplementary Fig. S3-4). A linear model based on S1_VH, strongest predictor, explained 33 % of the variation of SMC (R^2 = 0.33, RMSEcv = 16.0 %, Table 4 and Fig. 11-b). In mid summer, the predicting capacity decreased slightly (R^2 = 0.30, RMSEcv = 17.8 %, Table 4 and Fig. 11-d) based on a positive correlation between VMC and S2_NDMI (r = 0.55, p = 0.05). Although a significant correlation was observed between S2_NDVI and topographic slope and the SMC, the linear model constructed using S2_NDVI did not yield statistical significance (Table 4).
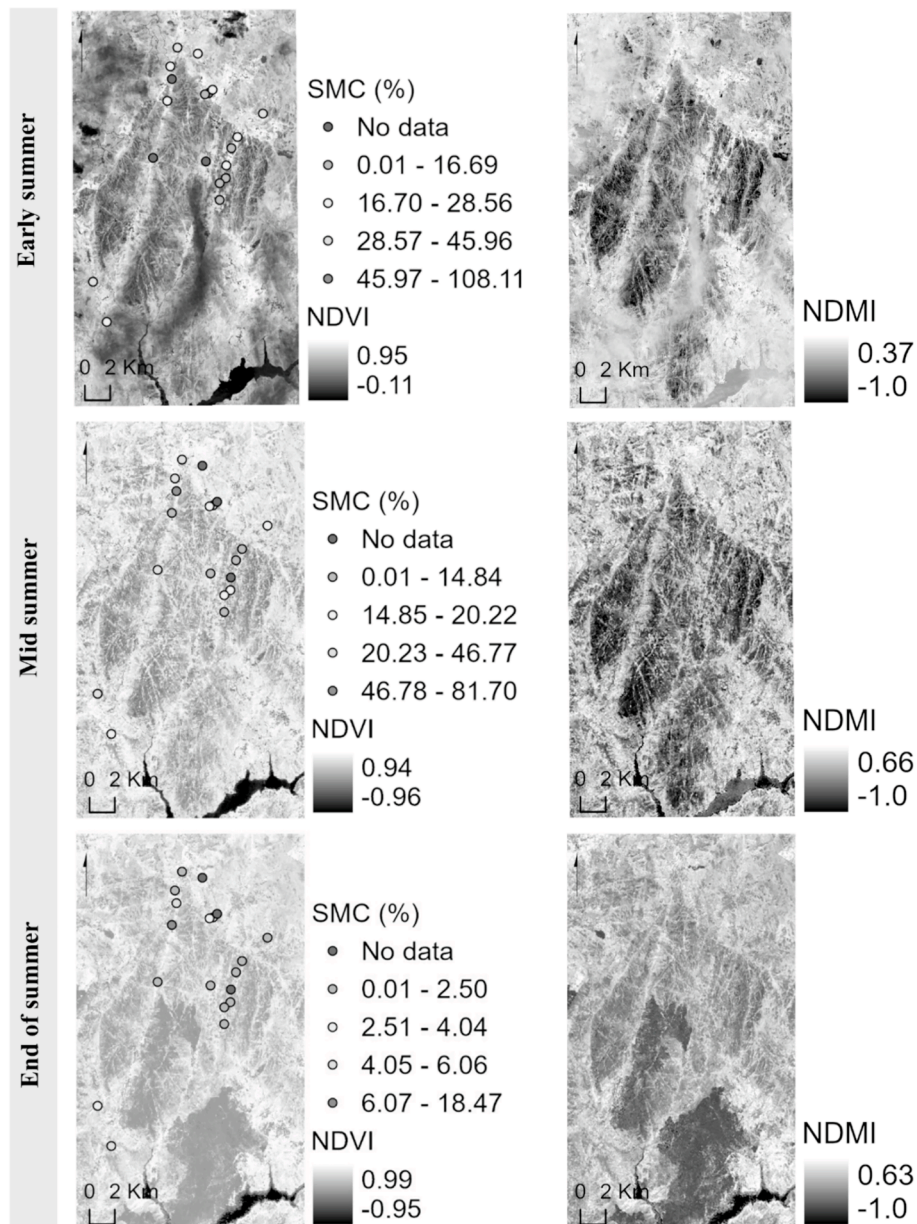
Fig. 8. Map showing the distribution of SMC (%) measured in the sampling sites in the early (6/07/2016), mid (12/07/2016), and end of summer (22/09/2016), and the NDVI and NDMI obtained from Sentinel-2 imagery for the 2nd June, 9th July and 20th September of 2016.

4. Discussion and conclusions

4.1. Remote sensing of vegetation and soil moisture content in Atlantic humid mountains

The aim of this exploratory study was to evaluate an empirical model that uses satellite-based predictors to estimate VMC and SMC in mountainous regions of the Southern European Atlantic, with this then providing a potential contribution to the management of landscape moisture dynamics. It is the first attempt to simultaneously investigate the use of S1 and S2 data for retrieving VMC and SMC, specifically in the Portuguese mountains. For that purpose, comparisons between field-measured VMC and SMC and S1 backscatter data and ratios and S2-derived optical indices were undertaken at landscape and vegetation type level, and across the season. The analyses were conducted in the summer season, where tools for assessing the VCM and SMC are most needed (Costa-Saura et al., 2021). The field measurements indicated

that vegetation was in average not stressed (median VMC = 80.5 %), but SMC values indicated soil drought in the top-layer (median SMC = 15.6 %), except in grasslands (median SMC = 28.6 %), where prevailed wet conditions. Within the vegetation types there was, however, large heterogeneity, a typical feature of Southern European Atlantic humid mountains.

4.1.1. Landscape vs vegetation type models

A pertinent question for the monitoring of VMC and SMC regards the spatial approach to follow, namely if a generalized landscape predictive model can be established, or if ecosystem specific models are needed to achieve better predictions. In general, our results showed that remote sensing of VMC and SMC remains challenging also in Atlantic humid mountains. While S1 and S2 predictors were significantly related VMC and SMC, the moderate predictive capacity of the models suggest caution in the use of these predictors to state moisture conditions in the vegetation and soil. Vegetation type models presented larger prediction
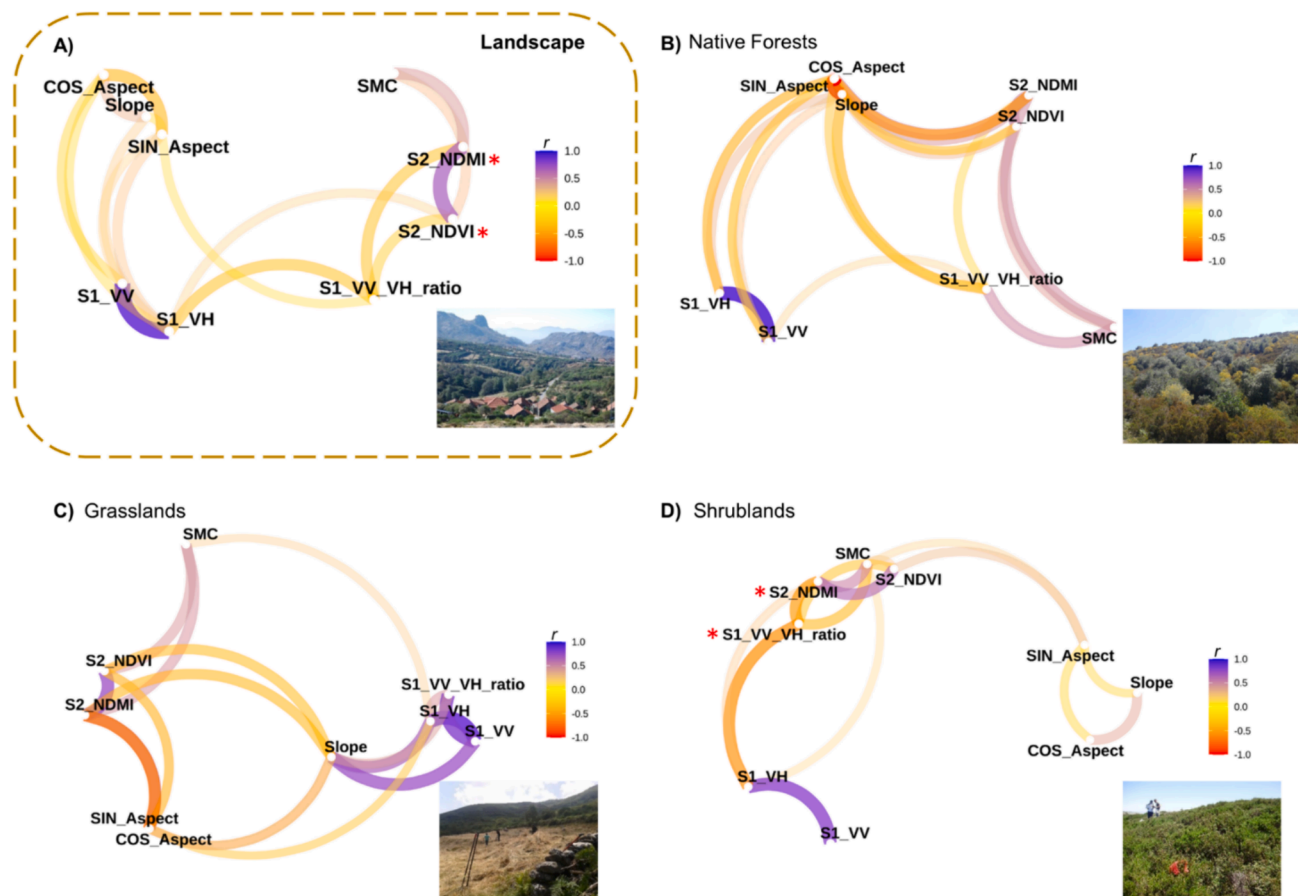
Fig. 9. Correlation network plot including all the Spearman correlations ® between soil moisture content (VMC) and the predictor variables at landscape level (full dataset (n = 48), A), and across each vegetation type (native forests (n = 15), B; and grasslands (n = 13), C, shrublands (n = 20), D). Predictor variables more highly correlated with SMC appear closer, joined by large path thickness coloured towards blue or red in case of positive or negative directions of the correlation, respectively. Predictor variables significantly associated with SMC (p < 0.05) are signed as *. (For interpretation of the references to colour in this figure legend, the reader is referred to the web version of this article.)

capacity than landscape models, particularly for VMC. Ecosystem specific models seems to be the most appropriate methodological pathway for spatially retrieving VMC and/or SMC. Best retrievals in VMC were obtained in shrublands and, to a lesser extent, in grasslands conditions. The variations explained by a model containing only shrublands or grasslands sites were 1.7 times and 1.2 times larger than from a landscape model (full dataset). This finding is congruent with previous studies that describe a decrease in model performance with the expansion of the range of vegetation conditions included in the VMC model (García et al., 2020; Rao et al., 2020) and also with the recent focus on specific vegetation type models (Lai et al., 2022). It also has implications for assessments that usually adopt satellite proxy variables to assess landscape VMC or introduce the effects of moisture in modelling frameworks. For SMC, our ecosystem-specific theory as the booster of model performance has less support, since only one vegetation type model was significant (i.e., shrublands) and with similar predictive capacity of the landscape model. SMC requires additional investigation in this regard.

The explained variance of our models was lower than in previous studies. The landscape model for VMC ($R^2 = 0.30$) was slightly below the 32.5 % of variation explained in Israel's Mediterranean ecosystems (Bar-Massada and Sviri, 2020), and far from the 55 % registered in Spain ($R^2 = 0.55$, Tanase et al., 2022) or the 69 % proposed in more arid and flat conditions in the south of Portugal (Santos et al., 2023). Our model results converged more when compared with previous studies undertaken at the vegetation type level, particularly in shrublands conditions. These studies also showed that VMC in shrublands is retrieved with

higher accuracy than in grasslands and woodlands (Costa-Saura et al., 2021; Yebra et al., 2013). The lack of a significant model for native forests and a generally poor performance in grasslands conditions corroborate such findings in this study. More than half of the variation of shrublands VMC was explained in our study ($R^2 = 0.52$), which is 17 % lower than reported in Mediterranean shrubland conditions over Spain ($R^2 = 0.70$, Costa-Saura et al., 2021; Yebra et al., 2013) or Southern United States ($R^2 = 0.69$, Lai et al., 2022). Indeed, considering cost-effective VMC models for Southern European Atlantic mountains, a shrublands model can be considered as the most promising. VMC maps of shrublands areas can be highly beneficial considering that such areas are the future forests and one of the most fire prone and abundant cover types in Mediterranean mountains (Moreira et al., 2009). The counter expectation was the weak results in grasslands conditions, as other studies showed a good association between VMC and satellite indices in grassland areas (Sow et al., 2013). Few comparative studies are available for grasslands (Davidson et al., 2006; Mendiguren et al., 2015; Sibanda et al., 2019), but our results were ($R^2 = 0.35$) substantially weak than the observed by Mendiguren et al., (2015) in Mediterranean dehesas when using MODIS data in South African grasslands with HyspIRI and EnMAP sensors ($R^2 = 0.59$, (Sibanda et al., 2019) or in the Canadian grasslands with Landsat data ($R^2 = 0.76$, Davidson et al., 2006). To what concerns SMC, significant models (landscape, $R^2 = 0.28$; shrublands, $R^2 = 0.31$) presented lower performance than that reported with S1 at the global level based on site-scale comparison ($R^2 = 0.53$, Mattia et al., 2018), in Mediterranean agroforestry conditions ($R^2 = 0.89$, Schönbrodt-Stitt et al., 2021), in the Himalayan Forelan ($R^2 =$
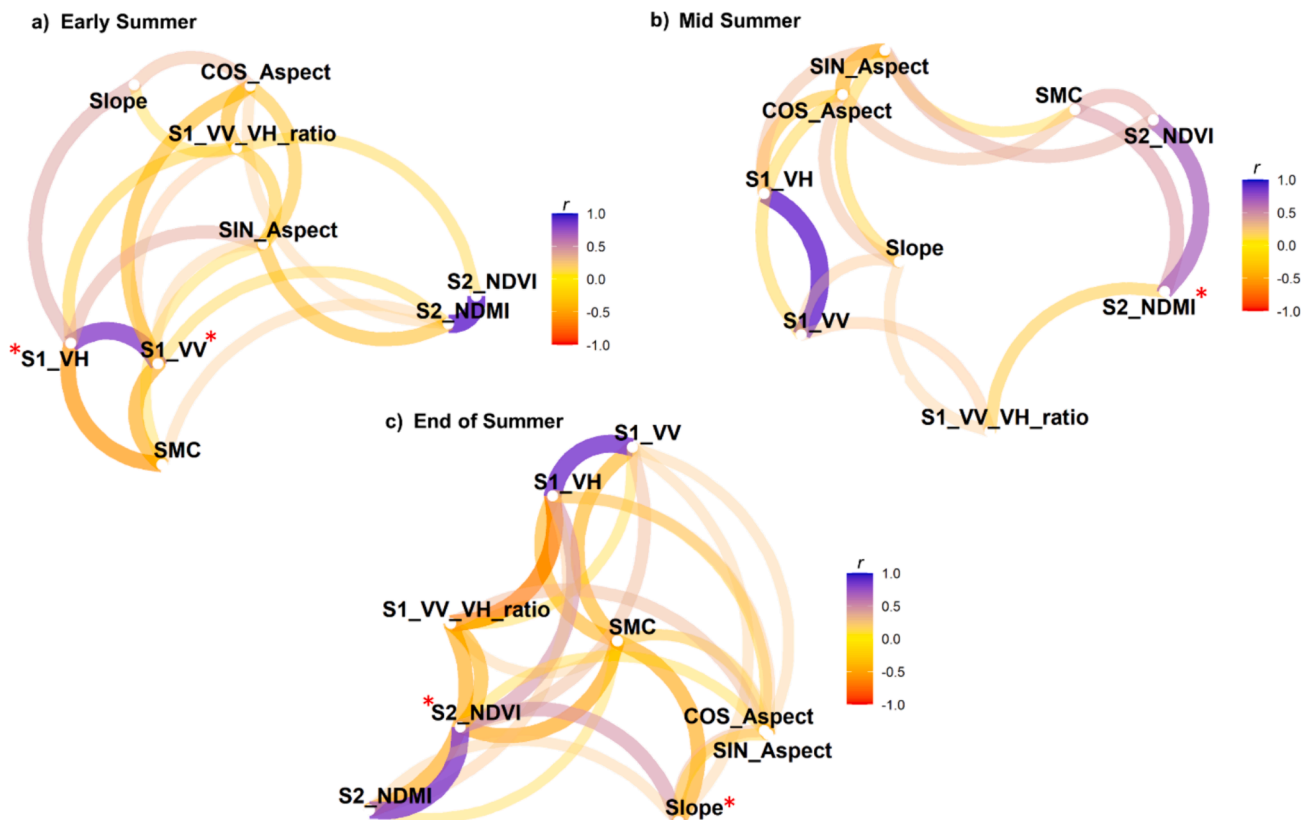
Fig. 10. Correlation network plot including all the Spearman correlation (*r*) between soil moisture content (SMC) and the set of predictor variables grouped by the season of data collection: early (6-7th June, n = 16), mid (12-13th July, n = 16) and end (21st-22nd September, n = 16) of summer 2016. Predictor variables more highly correlated with SMC appear closer, joined by large path thickness coloured towards blue or red in case of positive or negative directions of the correlation, respectively. Predictor variables significantly associated with SMC ($p < 0.05$) are signed as. (For interpretation of the references to colour in this figure legend, the reader is referred to the web version of this article.)

0.80, Singh and Gaurav, 2023) or in Chinese agricultural landscapes based in the synergetic use of S2 and S1 ($R^2 = 0.65$, Liang et al., 2021). The sensitivity of the S1 and S2 measurements to variations in SMC requires further investigations in Southern European Atlantic mountains.

4.1.2. Satellite-based predictors associated to VMC and SMC

Our mountainous context led us to hypothesize a topographic effect on the retrieval of VMC and SMC, and ancillary topographic variables were considered to act as control factors and improve model performance as shown by Schönbrodt-Stitt et al. (2021). No improvement of model performance with topographic control factors was found. The significant models found for VMC and SMC included always satellite predictors, indicating a role for Sentinel data in cost-effective predictive tools for these variables. Among the predictors for VMC, S2_NDMI and S2_NDVI were present in all significant models highlighting the relevance and importance of using optical satellite data. They related negatively and positively to VMC, respectively. The link and significance of S2_NDMI and S2_NDVI in quantifying VMC is in line with previous studies, which emphasized a more prominent role of the S2_NDMI than the S2_NDVI in the Mediterranean region (Bar-Massada and Sviri, 2020; Costa-Saura et al., 2021). Our results appear however to support a more important role of S2_NDVI, since it was always present in the best models for VMC. The relevant role of the NDVI aligns with previous findings in Mediterranean grassland–shrublands (Chuvieco et al., 2004). Nonetheless, the model with the largest explanation (shrublands) included S2 and S1 SAR predictors, namely the S1_VV backscatter coefficient. The combination of optical and SAR benefits the model estimations as demonstrated in other studies (Rao et al., 2020). S1_VV polarization showed an inverse relationship with VMC. For SMC,

S2_NMDI remained a relevant predictor, but results also emphasized the role of the S1 VV/VH ratio (S1_VV_VH_ratio) and S1_VH, both negatively associated to SMC. Previous studies observed the link of SMC with the S2_NDMI (Acharya et al., 2022), S1 VV/VH ratio (Nativel et al., 2022) and S1_VH (Rodionova, 2019). The negative association between SMC and S1_VH was also found in France (Rodionova, 2019) and in arid systems based on ground-based stations measurements (Ullmann et al., 2023). The S1 VV/VH ratio (S1_VV_VH_ratio) used by our study was less commonly used than S1 VH/VV ratio in soil moisture studies (Nativel et al., 2022; Ullmann et al., 2023; Vreugdenhil et al., 2020). VV/VH ratio was mostly applied in vegetation moisture content studies (Rao et al., 2020; Soudani et al., 2021b). Our results suggest further investigation of the S1 VV/VH ratio in soil moisture studies. S1 VV/VH ratio presented an inverse relationship with SMC as documented by Ullmann (Ullmann et al., 2023) for the S1 VH/VV ratio in arid conditions.

4.1.3. Variation of relationships during the summer season

The temporal portability of spectral approaches for estimating bio-physical attributes such as VMC or SMC must be assessed before they can be considered consistent predictive tools (Davidson et al., 2006). While our study is exploratory and do not have the necessary time-series evidence to argue on temporal portability, our results based on seasonal relationships (early summer, mid summer, end of summer) may provide initial insights in this regard. They highlighted a variation in the relationship between satellite predictors and VMC and SMC over the season. The intensity and the predictors associated with both moisture variables changed between the early and end of summer. For VMC and SMC, the end of the summer season was a time window where the link to spectral predictors was totally absent. This period coincided with the lowest values of VMC and SMC registered in this study. This time-scale
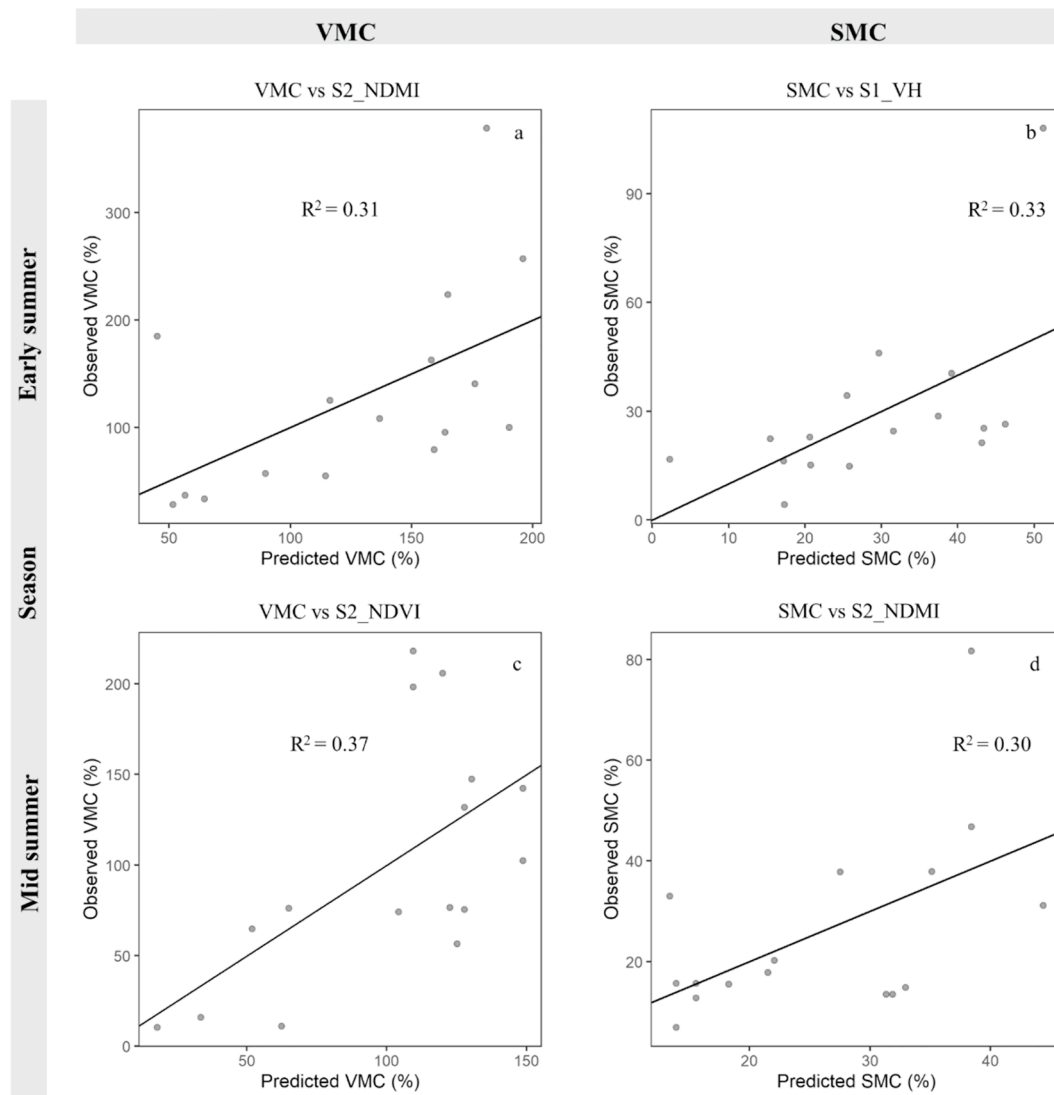
Fig. 11. Predicted and observed vegetation moisture content (VMC, %) and soil moisture content (SMC, %) using the regression models established with the predictors significantly correlated with VMC and SMC at each season (early summer, mid summer and end of summer). VMC and SMC predicted in the early summer using the S2_NDMI and S1_VH backscattering, respectively (a, b); (d). VMC and SMC predicted in the mid summer using the S2_NDVI and S2_NDMI, respectively (c, d). Coefficient of determination (R^2).

dependence was recently shown by Linscheid and colleagues (Linscheid et al., 2021) at an interannual time scale where the focus was on vegetation productivity based on satellite-based proxies. Soudani et al. (2021) also observed that, for the same LAI, the response of i.e. VV/VH differed depending on the phenological phase considered. Literature suggests that in the case of soil moisture, subsurface scattering may explain the lack of relationship between S1 and SMC (Wagner et al., 2022), because under dry soil conditions it reduces the sensitivity of backscatter to soil moisture. Overall, time-scale effects are one of challenges of integrating satellite remote sensing in ecosystem modelling at local scales (Pasetto et al., 2018) and empirical models for VMC and SMC need to account for seasonal sensitivities of moisture proxy variables (Linscheid et al., 2021). In Southern European Atlantic mountains particular attention should be taken in the late summer season.

4.2. Limitations

While this study made an effort to follow the best practices for using satellite data and derived measures for monitoring terrestrial ecosystems (Zeng et al., 2022), a number of limitations must be highlighted. First,

the field data collection is limited to three collection dates over the summer. Second, the sample values in each collection date were based on a single measurement inside the plot (20×20 m), not measuring i.e. VMC or SMC at species level. Our VMC and SMC values are however in line with those reported in similar studies (Chuvieco et al., 2004; Costa-Saura et al., 2021; de Figueiredo et al., 2021; García et al., 2020; Tanase et al., 2022; Yebra et al., 2013). At modelling, the small sample size limited the construction of more complex models at vegetation type and at seasonal level. It is likely an improvement of predictive capacity for VMC and SMC with more complex models. We have indications that a more accurate model would be achievable with a bigger sample size, at least based on the early summer VMC model where two meaningful independent predictors were found. Despite that, efforts to improve model performance were performed, namely by including topographic control factors (discussed above), and by in parallel evaluating regression models using relativized spectral indexes (data not shown, García et al., 2020) or different curve fitting (i.e. exponential, quadratic; Liang et al., 2021). We did not find a model improvement through these strategies. Overall, with assumed limitations, this study brings important insights for satellite landscape management of vegetation and soil

moisture in the Southern European Atlantic mountains. This and other similar regions are facing increasing challenges due to climate change (Zapata-Sierra et al., 2022), European policies concerning water management (Commission, 2021) and there is an increasing need for local communities to adapt to the evolving mountain environment (Castro et al., 2021). Further improvement in VMC and SMC prediction may be achieved by including meteorological control factors from local weather observations (Costa-Saura et al., 2021), intensifying sampling efforts, and testing the effect of plot vs moving window values for the predictors in order to evaluate uncertainty rising from misregistration between plot and reference pixels.

CRediT authorship contribution statement

Antonio T. Monteiro: Conceptualization, Data curation, Formal analysis, Methodology, Project administration, Writing – original draft. **Salvador Arenas-Castro:** Conceptualization, Data curation, Methodology, Writing – original draft, Writing – review & editing. **Suvarna M. Punalekar:** Writing – original draft, Writing – review & editing. **Mário Cunha:** Formal analysis, Methodology, Writing – original draft, Writing – review & editing. **Inès Mendes:** Writing – original draft, Writing – review & editing. **Mariasilvia Giamberini:** Writing – original draft, Writing – review & editing. **Eduarda Marques da Costa:** Writing – original draft, Writing – review & editing. **Francesco Fava:** Methodology, Writing – original draft, Writing – review & editing. **Richard Lucas:** Methodology, Supervision, Writing – original draft, Writing – review & editing.

Declaration of competing interest

The authors declare that they have no known competing financial interests or personal relationships that could have appeared to influence the work reported in this paper.

Data availability

Data will be made available on request.

Acknowledgements

Appendix A. Supplementary data

Supplementary data to this article can be found online at https://doi.org/10.1016/j.ecolind.2024.112123.

References

Acharya, U., Daigh, A.L.M., Oduor, P.G., 2022. Soil moisture mapping with moisture-related indices, OPTRAM, and an integrated random forest-OPTRAM algorithm from Landsat 8 images. Remote Sens. (Basel) 14, 3801.

Airbus, D., 2020. Copernicus DEM Copernicus Digital Elevation Model Validation Report. Airbus Defence and Space—Intelligence: Potsdam, Germany.

Atmosfera, I.P.d.M.e., 2016. Boletim climatológico de Portugal Continental- Maio de 2016, in: IPMA (Ed.).

Bar-Massada, A., Sviri, A., 2020. Utilizing vegetation and environmental new micro spacecraft (VENµS) data to estimate live fuel moisture content in Israel's Mediterranean Ecosystems. IEEE J. Sel. Top. Appl. Earth Obs. Remote Sens. 13, 3204–3212.

Bauer-Marschallinger, B., Freeman, V., Cao, S., Paulik, C., Schaufler, S., Stachl, T., Modanesi, S., Massari, C., Ciabatta, L., Brocca, L.L., Wagner, W., 2019. Toward global soil moisture monitoring with Sentinel-1: harnessing assets and overcoming obstacles. IEEE Trans. Geosci. Remote Sens. 57, 520–539.

Benninga, H.-J.-F., van der Velde, R., Su, Z., 2020. Sentinel-1 soil moisture content and its uncertainty over sparsely vegetated fields. J. Hydrol. X 9, 100066.

Brown, T.P., Hoylman, Z.H., Conrad, E., Holden, Z., Jencso, K., Jolly, W.M., 2022. Decoupling between soil moisture and biomass drives seasonal variations in live fuel moisture across co-occurring plant functional types. Fire Ecology 18, 14.

Calheiros, T., Benali, A., Pereira, M., Silva, J., Nunes, J., 2022. Drivers of extreme burnt area in Portugal: fire weather and vegetation. Nat. Hazards Earth Syst. Sci. 22, 4019–4037.

Carvalho-Santos, C., Nunes, J.P., Monteiro, A.T., Hein, L., Honrado, J.P., 2016. Assessing the effects of land cover and future climate conditions on the provision of hydrological services in a medium-sized watershed of Portugal. Hydrol. Process. 30, 720–738.

Carvalho-Santos, C., Monteiro, A.T., Arenas-Castro, S., Greifeneder, F., Marcos, B., Portela, A.P., Honrado, J.P., 2018. Ecosystem services in a protected mountain range of Portugal: satellite-based products for state and trend analysis. Remote Sens. (Basel) 10, 1573.

Castro, J., Castro, M., Gómez-Sal, A., 2021. Changes on the Climatic Edge: Adaptation of and Challenges to Pastoralism in Montesinho (Northern Portugal). Mountain Research and Development 41.

Choler, P., 2023. Above-treeline ecosystems facing drought: lessons from the 2022 European summer heat wave. Biogeosciences 20, 4259–4272.

Chuvieco, E., Cocero, D., Riaño, D., Martin, P., Martínez-Vega, J., de la Riva, J., Pérez, F., 2004. Combining NDVI and surface temperature for the estimation of live fuel moisture content in forest fire danger rating. Remote Sens. Environ. 92, 322-331.

Commission, E., 2021. Communication from the commission to the European Parliament, the council, the European Economic and Social Committee and the Committee of the regions: New EU Forest Strategy for 2030, COM (2021) 572, final ed. European Commission, Brussels.

Costa-Saura, J.M., Balaguer-Beser, Á., Ruiz, L.A., Pardo-Pascual, J.E., Soriano-Sancho, J. L., 2021. Empirical models for spatio-temporal live fuel moisture content estimation in mixed Mediterranean vegetation areas using Sentinel-2 indices and meteorological data. Remote Sens. (Basel) 13, 3726.

Davidson, A., Wang, S., Wilmshurst, J., 2006. Remote sensing of grassland–shrubland vegetation water content in the shortwave domain. Int. J. Appl. Earth Obs. Geoinf. 8, 225–236.

de Figueiredo, T., Royer, A.C., Fonseca, F., de Araújo Schütz, F.C., Hernández, Z., 2021. Regression models for soil water storage estimation using the ESA CCI satellite soil moisture product: A case study in Northeast Portugal. Water 13, 37.

Devadoss, J., Falco, N., Dafflon, B., Wu, Y., Franklin, M., Hermes, A., Hinckley, E.-L.-S., Wainwright, H., 2020. Remote sensing-informed zonation for understanding snow, plant and soil moisture dynamics within a mountain ecosystem. Remote Sens. (Basel) 12, 2733.

Drenkhan, F., Buytaert, W., Mackay, J.D., Barrand, N.E., Hannah, D.M., Huggel, C., 2023. Looking beyond glaciers to understand mountain water security. Nat. Sustainability 6, 130–138.

El Hajj, M., Baghdadi, N., Zribi, M., Bazzi, H., 2017. Synergic use of Sentinel-1 and Sentinel-2 images for operational soil moisture mapping at high spatial resolution over agricultural areas. Remote Sens. (Basel) 9, 1292.

Fava, F., Colombo, R., Bocchi, S., Meroni, M., Sitzia, M., Fois, N., Zucca, C., 2009. Identification of hyperspectral vegetation indices for Mediterranean pasture characterization. Int. J. Appl. Earth Obs. Geoinf. 11, 233–243.

Feldman, A.F., Short Gianotti, D.J., Dong, J., Akbar, R., Crow, W.T., McColl, K.A., Konings, A.G., Nippert, J.B., Tumber-Dávila, S.J., Holbrook, N.M., Rockwell, F.E., Scott, R.L., Reichle, R.H., Chatterjee, A., Joiner, J., Poulter, B., Entekhabi, D., 2023. Remotely sensed soil moisture can capture dynamics relevant to plant water uptake. Water Resour. Res. 59, e2022WR033814.

Fieberg, J., Johnson, D.H., 2015. MMI: Multimodel inference or models with management implications? J. Wildl. Manag. 79, 708–718.

Forkel, M., Schmidt, L., Zotta, R.M., Dorigo, W., Yebra, M., 2023. Estimating leaf moisture content at global scale from passive microwave satellite observations of vegetation optical depth. Hydrol. Earth Syst. Sci. 27, 39–68.

García, M., Riaño, D., Yebra, M., Salas, J., Cardil, A., Monedero, S., Ramirez, J., Martín, M.P., Vilar, L., Gajardo, J., Ustin, S., 2020. A live fuel moisture content product from Landsat TM satellite time series for implementation in fire behavior models. Remote Sens. (Basel) 12, 1714.

Gómez-Giráldez, P.J., Aguilar, C., Polo, M.J., 2014. Natural vegetation covers as indicators of the soil water content in a semiarid mountainous watershed. Ecol. Ind. 46, 524–535.

Gomis-Cebolla, J., Garcia-Arias, A., Perpinyà-Vallès, M., Francés, F., 2022. Evaluation of Sentinel-1, SMAP and SMOS surface soil moisture products for distributed eco-hydrological modelling in Mediterranean forest basins. J. Hydrol. 608, 127569.

Greifeneder, F., Notarnicola, C., Wagner, W., 2021. A machine learning-based approach for surface soil moisture estimations with Google earth engine. Remote Sens. (Basel) 13, 2099.

Holzman, M., Rivas, R., Carmona, F., Niclòs, R., 2017. A method for soil moisture probes calibration and validation of satellite estimates. MethodsX 4, 243–249.

Jackson, T.J., Schmugge, T.J., O'Neill, P., 1984. Passive microwave remote sensing of soil moisture from an aircraft platform. Remote Sens. Environ. 14, 135–151.

Konings, A.G., Saatchi, S.S., 2021. Detecting forest response to droughts with global observations of vegetation water content. 27, 6005–6024.

Lai, G., Quan, X., Yebra, M., He, B., 2022. Model-driven estimation of closed and open shrublands live fuel moisture content. Giscience & Remote Sensing 59, 1837–1856.

Lehmann, A., Masò, J., Nativi, S., Giuliani, G., 2020. Towards integrated essential variables for sustainability. Int. J. Digital Earth 13, 158–165.

Liang, J., Liang, G., Zhao, Y., Zhang, Y., 2021. A synergic method of Sentinel-1 and Sentinel-2 images for retrieving soil moisture content in agricultural regions. Comput. Electron. Agric. 190, 106485.

Linscheid, N., Mahecha, M.D., Rammig, A., Carvalhais, N., Gans, F., Nelson, J.A., Walther, S., Weber, U., Reichstein, M., 2021. Time-scale dependent relations between earth observation based proxies of vegetation productivity. Geophys. Res. Lett. 48, e2021GL093285.

Mattia, F., Balenzano, A., Satalino, G., Lovergine, F., Peng, J., Wegmuller, U., Cartus, O., Davidson, M.W.J., Kim, S., Johnson, J., Walker, J., Wu, X., Pauwels, V.R.N., McNairn, H., Caldwell, T., Cosh, M., Jackson, T., 2018. Sentinel-1 & Sentinel-2 for SOIL Moisture Retrieval at Field Scale, IGARSS 2018 - 2018 IEEE International Geoscience and Remote Sensing Symposium, pp. 6143-6146.

Mendiguren, G., Pilar Martín, M., Nieto, H., Pacheco-Labrador, J., Jurdao, S., 2015. Seasonal variation in grass water content estimated from proximal sensing and MODIS time series in a Mediterranean Fluxnet site. Biogeosciences 12, 5523–5535.

Meyer, H., Lehnert, L.W., Wang, Y., Reudenbach, C., Nauss, T., Bendix, J., 2017. From local spectral measurements to maps of vegetation cover and biomass on the Qinghai-Tibet-Plateau: Do we need hyperspectral information? Int. J. Appl. Earth Obs. Geoinf. 55, 21–31.

Monteiro, A.T., Fava, F., Gonçalves, J., Huete, A., Gusmeroli, F., Parolo, G., Spano, D., Bocchi, S., 2013. Landscape context determinants to plant diversity in the permanent meadows of Southern European Alps. Biodivers. Conserv. 22, 937–958.

Monteiro, A.T., Carvalho-Santos, C., Lucas, R., Rocha, J., Costa, N., Giamberini, M., Costa, E.M.d., Fava, F., 2021. Progress in grassland cover conservation in Southern European Mountains by 2020: A transboundary assessment in the Iberian Peninsula with satellite observations (2002–2019). Remote Sens. (Basel) 13, 3019.

Moreira, F., Vaz, P., Catry, F., Silva, J., 2009. Regional variations in wildfire susceptibility of land-cover types in Portugal: implications for landscape management to minimize fire hazard. Int. J. Wildland Fire 18, 563–574.

Nativel, S., Ayari, E., Rodriguez-Fernandez, N., Baghdadi, N., Madelon, R., Albergel, C., Zribi, M., 2022. Hybrid methodology using Sentinel-1/Sentinel-2 for soil moisture estimation. Remote Sens. (Basel) 14, 2434.

Pace, G., Gutiérrez-Cánovas, C., Henriques, R., Boeing, F., Cássio, F., Pascoal, C., 2021. Remote sensing depicts riparian vegetation responses to water stress in a humid Atlantic region. Sci. Total Environ. 772, 145526.

Pasetto, D., Arenas-Castro, S., Bustamante, J., Casagrandi, R., Chrysoulakis, N., Cord, A. F., Dittrich, A., Domingo-Marimon, C., El Serafy, G., Karnieli, A., Kordelas, G.A., Manakos, I., Mari, L., Monteiro, A., Palazzi, E., Poursanidis, D., Rinaldo, A., Terzago, S., Ziemba, A., Ziv, G., 2018. Integration of satellite remote sensing data in ecosystem modelling at local scales: Practices and trends. Methods Ecol Evol 9, 1810–1821.

Pôças, I., Cunha, M., Marcal, A.R.S., Pereira, L.S., 2011. An evaluation of changes in a mountainous rural landscape of Northeast Portugal using remotely sensed data. Landsc. Urban Plan. 101, 253–261.

Pôças, I., Cunha, M., Pereira, L.S., Allen, R.G., 2013. Using remote sensing energy balance and evapotranspiration to characterize montane landscape vegetation with focus on grass and pasture lands. Int. J. Appl. Earth Obs. Geoinf. 21, 159–172.

QGISTeam, 2022. QGIS Geographic Information System, 3.24 ed. QGIS Association.

Rao, K., Williams, A.P., Flefil, J.F., Konings, A.G., 2020. SAR-enhanced mapping of live fuel moisture content. Remote Sens. Environ. 245, 111797.

Rivas-Martínez, S., Penas, Á., del Río, S., Díaz González, T.E., Rivas-Sáenz, S., 2017. Bioclimatology of the Iberian Peninsula and the Balearic Islands. In: Loidi, J. (Ed.), The Vegetation of the Iberian Peninsula, Volume 1. Springer International Publishing, Cham, pp. 29–80.

Rodionova, N.V., 2019. Correlation of the Sentinel 1 Radar data with ground-based measurements of the soil temperature and moisture. Izv. Atmos. Ocean. Phys. 55, 939–948.

Rodriguez-Jimenez, F., Lorenzo, H., Novo, A., Acuña-Alonso, C., Alvarez, X., 2023. Modelling of live fuel moisture content in different vegetation scenarios during dry periods using meteorological data and spectral indices. For. Ecol. Manage. 546, 121378.

RStudioTeam, 2020. RStudio: Integrated Development for R., in: RStudio (Ed.), PBC, Boston, MA.

Santi, E., Paloscia, S., Pettinato, S., Fontanelli, G., 2016. Application of artificial neural networks for the soil moisture retrieval from active and passive microwave spaceborne sensors. Int. J. Appl. Earth Obs. Geoinf. 48, 61–73.

Santos, F.L.M., Couto, F.T., Dias, S.S., Ribeiro, N.A., Salgado, R., 2023. Vegetation fuel characterization using machine learning approach over southern Portugal. Remote Sensing Applications: Society and Environment, 101017.

Schlund, M., Erasmi, S., 2020. Sentinel-1 time series data for monitoring the phenology of winter wheat. Remote Sens. Environ. 246, 111814.

Schönbrodt-Stitt, S., Ahmadian, N., Kurtenbach, M., Conrad, C., Romano, N., Bogena, H. R., Vereecken, H., Nasta, P., 2021. Statistical Exploration of SENTINEL-1 Data, Terrain Parameters, and in-situ Data for Estimating the Near-Surface Soil Moisture in a Mediterranean Agroecosystem. Frontiers in Water 3.

Sibanda, M., Mutanga, O., Dube, T., Mothapo, M.C., Mafongoya, P.L., 2019. Remote sensing equivalent water thickness of grass treated with different fertiliser regimes using resample HyspIRI and EnMAP data. Phys. Chem. Earth Parts A/B/C 112, 246–254.

Singh, A., Gaurav, K., 2023. Deep learning and data fusion to estimate surface soil moisture from multi-sensor satellite images. Sci. Rep. 13, 2251.

Soudani, K., Delpierre, N., Berveiller, D., Hmimina, G., Vincent, G., Morfin, A., Dufrêne, É., 2021. Potential of C-band Synthetic Aperture Radar Sentinel-1 time-series for the monitoring of phenological cycles in a deciduous forest. Int. J. Appl. Earth Obs. Geoinf. 104, 102505.

Sow, M., Mbow, C., Hély, C., Fensholt, R., Sambou, B., 2013. Estimation of herbaceous fuel moisture content using vegetation indices and land surface temperature from MODIS data. Remote Sens. (Basel) 5, 2617–2638.

Tanase, M.A., Nova, J.P.G., Marino, E., Aponte, C., Tomé, J.L., Yáñez, L., Madrigal, J., Guijarro, M., Hernando, C., 2022. Characterizing live fuel moisture content from active and passive sensors in a Mediterranean environment. Forests 13, 1846.

Ullmann, T., Jagdhuber, T., Hoffmeister, D., May, S.M., Baumhauer, R., Bubenzer, O., 2023. Exploring Sentinel-1 backscatter time series over the Atacama Desert (Chile) for seasonal dynamics of surface soil moisture. Remote Sens. Environ. 285, 113413.

Vij, S., Biesbroek, R., Adler, C., Muccione, V., 2021. Climate Change Adaptation in European Mountain Systems: A Systematic Mapping of Academic Research. Mountain Research and Development 41.

Vreugdenhil, M., Wagner, W., Bauer-Marschallinger, B., Pfeil, I., Teubner, I., Rüdiger, C., Strauss, P., 2018. Sensitivity of Sentinel-1 Backscatter to Vegetation Dynamics: An Austrian Case Study, Remote Sensing.

Vreugdenhil, M., Navacchi, C., Bauer-Marschallinger, B., Hahn, S., Steele-Dunne, S., Pfeil, I., Dorigo, W., Wagner, W., 2020. Sentinel-1 Cross Ratio and Vegetation Optical Depth: A Comparison over Europe, Remote Sensing.

Wagner, W., Lindorfer, R., Melzer, T., Hahn, S., Bauer-Marschallinger, B., Morrison, K., Calvet, J.-C., Hobbs, S., Quast, R., Greimeister-Pfeil, I., Vreugdenhil, M., 2022. Widespread occurrence of anomalous C-band backscatter signals in arid environments caused by subsurface scattering. Remote Sens. Environ. 276, 113025.

Wang, Q., Jin, T., Li, J., Chang, X., Li, Y., Zhu, Y., 2022. Modeling and assessment of vegetation water content on soil moisture retrieval via the synergistic use of Sentinel-1 and Sentinel-2. Earth Space Sci. 9, e2021EA002063.

Wenger, S.J., Olden, J.D., 2012. Assessing transferability of ecological models: an underappreciated aspect of statistical validation. Methods Ecol Evol 3, 260–267.

Yebra, M., Dennison, P.E., Chuvieco, E., Riaño, D., Zylstra, P., Hunt, E.R., Danson, F.M., Qi, Y., Jurdao, S., 2013. A global review of remote sensing of live fuel moisture content for fire danger assessment: Moving towards operational products. Remote Sens. Environ. 136, 455–468.

Zapata-Sierra, A.J., Zapata-Castillo, L., Manzano-Agugliaro, F., 2022. Water resources availability in southern Europe at the basin scale in response to climate change scenarios. Environ. Sci. Eur. 34, 75.

Zeng, Y., Hao, D., Huete, A., Dechant, B., Berry, J., Chen, J.M., Joiner, J., Frankenberg, C., Bond-Lamberty, B., Ryu, Y., Xiao, J., Asrar, G.R., Chen, M., 2022. Optical vegetation indices for monitoring terrestrial ecosystems globally. Nat. Rev. Earth Environ. 3, 477–493.